A STRUCTURED PSEUDOSPECTRAL METHOD FOR $\mathcal{H}_\infty$-NORM COMPUTATION OF LARGE-SCALE DESCRIPTOR SYSTEMS

PETER BENNER* AND MATTHIAS VOIGT*,†

Abstract. In this paper we discuss the problem of computing the $\mathcal{H}_\infty$-norm of transfer functions associated to large-scale descriptor systems. We exploit the relationship between the $\mathcal{H}_\infty$-norm and the structured complex stability radius of a corresponding matrix pencil. To compute the structured stability radius we consider so-called structured pseudospectra. Namely, we have to find the pseudospectrum touching the imaginary axis. Therefore, we set up an iteration over the real part of the rightmost pseudoeigenvalue. For that we use a new fast iterative scheme which is based on certain rank-1 perturbations of a matrix pencil. Finally, we analyze the performance of our algorithm by using real-world examples. In particular we compare our method with different other algorithms including a recently and independently derived method from Guglielmi, Gürbüzbalaban, and Overton.

Key words. Descriptor systems, $\mathcal{H}_\infty$ control, iterative methods, pseudospectra, sparse matrices, stability of linear systems.

1. Introduction. In this paper we consider linear time-invariant descriptor systems of the form

$$\begin{aligned} E\dot{x}(t) &= Ax(t) + Bu(t), \\ y(t) &= Cx(t) + Du(t), \end{aligned} \tag{1.1}$$

where E, $A \in \mathbb{R}^{n\times n}$, $B \in \mathbb{R}^{n\times m}$, $C \in \mathbb{R}^{p\times n}$, $D \in \mathbb{R}^{p\times m}$, $x(t) \in \mathbb{R}^n$ is the descriptor vector, $u(t) \in \mathbb{R}^m$ is the input vector, and $y(t) \in \mathbb{R}^p$ is the output vector. Systems of this kind are the natural formulation of many dynamical models arising, e.g., in the simulation, control and optimization of electrical circuits [38–40], constrained multibody systems [20, 36], or certain semidiscretized PDEs [2, 27, 47]. The $\mathcal{H}_\infty$-norm is a popular tool to measure the distance of dynamical systems which is of importance, e.g., as an error measure in model order reduction, see [27, 36] and references therein. Another application can be found in robust stability analysis and robust control [49] as a robustness measure. This paper presents a new numerical method to compute this norm for *large-scale* systems based on optimizing over structured pseudospectra.

Throughout this paper we assume that $\lambda E - A$ is a *regular* matrix pencil, i.e., $\det(\lambda E - A) \not\equiv 0$. Furthermore, we assume that all involved matrices are large and sparse with m, $p \ll n$. We will call a descriptor system *asymptotically stable* if $\Lambda_\mathrm{f}(E, A) \subset \mathbb{C}^- := \{s \in \mathbb{C} : \mathrm{Re}\,(s) < 0\}$, where $\Lambda_\mathrm{f}(E, A)$ is the set of all finite eigenvalues of $\lambda E - A$. For brevity we will just call such a system stable since we exclude eigenvalues on the imaginary axis.

Instead of working in the time domain, we often turn to the Laplace domain. By taking the Laplace transforms of both equations in (1.1) and assuming $Ex(0) = 0$ we obtain the transfer function [16]

$$G(s) = C(sE - A)^{-1}B + D. \tag{1.2}$$

Throughout the whole paper we assume w.l.o.g. that $D = 0$. Otherwise we could

*Max Planck Institute for Dynamics of Complex Technical Systems, Sandtorstr. 1, 39106 Magdeburg, Germany (benner@mpi-magdeburg.mpg.de, voigtm@mpi-magdeburg.mpg.de).

†Corresponding author, phone: +49 391 6110 450, fax: +49 391 6110 453.

Appears in *Mathematics of Control, Signals, and Systems* (©Springer-Verlag London)

rewrite (1.2) as

$$G(s) = \begin{bmatrix} C & I_p \end{bmatrix} \left(s \begin{bmatrix} E & 0 \\ 0 & 0 \end{bmatrix} - \begin{bmatrix} A & 0 \\ 0 & -I_p \end{bmatrix} \right)^{-1} \begin{bmatrix} B \\ D \end{bmatrix} \tag{1.3}$$

to achieve this form. Summarizing, we will restrict ourselves to the class of systems

$$\begin{aligned} E\dot{x}(t) &= Ax(t) + Bu(t), \\ y(t) &= Cx(t), \end{aligned} \tag{1.4}$$

which we will sometimes denote by $\Sigma = (\lambda E - A, B, C)$ with associated transfer function

$$G(s) = C(sE - A)^{-1}B. \tag{1.5}$$

We call $G(\cdot)$ *(asymptotically) stable* if all its *finite* poles are located in the open left half-plane, i.e., $\Pi_{\mathrm{f}}(E, A, B, C) \subset \mathbb{C}^-$, where $\Pi_{\mathrm{f}}(E, A, B, C)$ denotes the set of all finite poles of $G(\cdot)$. Furthermore, we call $G(\cdot)$ *proper* if $\lim_{\omega\to\infty} \|G(\mathrm{i}\omega)\|_2 < \infty$ (with $\|\cdot\|_2$ denoting the spectral norm of a matrix), otherwise we call it *improper*. By $\mathcal{RH}_\infty^{p\times m}$ we denote the rational Banach space of all stable and proper functions of the form (1.5), see, e.g., [49]. For this space we define the $\mathcal{H}_\infty$*-norm*, given by

$$\|G\|_{\mathcal{H}_\infty} := \sup_{s\in\mathbb{C}^+} \sigma_{\max}(G(s)) = \sup_{\omega\in\mathbb{R}} \sigma_{\max}(G(\mathrm{i}\omega)),$$

with $\mathbb{C}^+ := \{s \in \mathbb{C} : \mathrm{Re}\,(s) > 0\}$ and the maximum singular value $\sigma_{\max}(\cdot)$. Our aim is to compute this norm value under the assumptions stated above.

Numerical methods for computing the $\mathcal{H}_\infty$-norm have been known for a long time. Most of them are based on relations between the $\mathcal{H}_\infty$-norm and the spectrum of certain Hamiltonian matrices or pencils. For an overview, we refer to [3,4,7–9,11]. We briefly summarize the most general result presented in [3]. Under some assumptions it holds that $\|G\|_{\mathcal{H}_\infty} < \gamma$ if and only if the *skew-Hamiltonian/Hamiltonian matrix pencil* [1]

$$\lambda\mathcal{S} - \mathcal{H}_\gamma = \lambda \begin{bmatrix} E & 0 \\ 0 & E^T \end{bmatrix} - \begin{bmatrix} A & \frac{1}{\gamma}BB^T \\ -\frac{1}{\gamma}C^TC & -A^T \end{bmatrix}$$

has no finite, purely imaginary eigenvalues. Based on that, the algorithm chooses an initial guess $\gamma < \|G\|_{\mathcal{H}_\infty}$ and iterates over γ in a suitable way until $\lambda\mathcal{S} - \mathcal{H}_\gamma$ has no finite, purely imaginary eigenvalues. This iteration can be implemented in a globally quadratically converging way. The drawback of the algorithm is the decision in each step whether there are purely imaginary eigenvalues. It is important to find *all* of them since otherwise the algorithm could fail. In [3] this issue was addressed by using a structure-preserving method for $\lambda\mathcal{S}-\mathcal{H}_\gamma$, which prevents the finite, purely imaginary eigenvalues to move off the imaginary axis as long as their pairwise distance is sufficiently large [1]. However, this method computes a full structured factorization of the pencil in each step. Due to its cubic complexity it is infeasible for large-scale problems. We could consider a closely related extended *even matrix pencil* and try to compute the desired eigenvalues close to a specified shift with the method presented in [35]. However, the question remains how to reliably compute *all* finite, purely imaginary eigenvalues. Another approach presented in [13, 14] uses the so-called bounded real lemma to estimate the $\mathcal{H}_\infty$-norm of a discrete-time state-space system which is required to be given in a minimal realization [16]. This algorithm

checks a sequence of linear matrix inequalities for feasibility. This is done by deciding if a so-called Chandrasekhar iteration converges. However, this test lacks of reliability, in particular if the iterates are approaching the $\mathcal{H}_\infty$-norm. Hence, only an estimation of the norm value can be given by this algorithm. Therefore, in this paper we use another approach based on pseudospectra. Independently from and in parallel to our derivation, a similar basic idea has been used in [22] to develop a method for $\mathcal{H}_\infty$-norm computation. The main differences are that our approach allows the treatment of descriptor systems, i.e., systems with singular E, and extends the definition of the complex stability radius by incorporating the infinite poles of the system. We also use a different optimization procedure to drive the pseudospectral abscissa to zero. We will discuss these differences in more detail at the end of the paper. We have already presented part of this work in [5]. However, in this paper we include some new features from [22], all proofs and a more detailed discussion of numerical examples. In particular, we generalize the Newton-based approach from [22] to optimize the structured pseudospectral abscissa. This method gives a slightly better performance than the secant-type method used in [6].

Our paper is structured as follows. In Section 2 we introduce the basic terminology and concepts that we will make use of in this work. Furthermore, we briefly discuss some applications of the $\mathcal{H}_\infty$-norm. Results on the relationship between the $\mathcal{H}_\infty$-norm and the structured complex stability radius for descriptor systems are discussed in Section 3. In Section 4 we describe how to compute the so-called structured pseudospectral abscissa of a transfer function which is the key ingredient of this paper. A large part of this section will also be devoted to fixed point analysis. In Section 5 we describe how to use Newton's method to compute the structured stability radius of the system. Section 6 is devoted to the analysis of the differences between this paper and the reference [22] since both are based on similar ideas. In particular, we show that both methods are *not* equivalent in the context of standard state-space systems. In Section 7 we present a study of numerical examples. In particular, we compare our method with existing algorithms. Furthermore, we analyze drawbacks and limitations. Finally, in Section 8 we give conclusions and point towards possible future research directions.

2. Mathematical Preliminaries and Applications. In the sequel we need the following concepts and terminology. A regular matrix pencil $\lambda E - A$ can be reduced to *Weierstraß canonical form* [31]

$$E = W \begin{bmatrix} I_{n_\mathrm{f}} & 0 \\ 0 & N \end{bmatrix} T, \quad A = W \begin{bmatrix} J & 0 \\ 0 & I_{n_\infty} \end{bmatrix} T, \tag{2.1}$$

where W and T are nonsingular, I_k is an identity matrix of order k, J and N are in Jordan canonical form and N is nilpotent with index of nilpotency ν. The number ν is also called the *algebraic index* of the descriptor system (1.4) and n_f and n_∞ are the dimensions of the deflating subspaces of $\lambda E - A$ corresponding to the finite and infinite eigenvalues, respectively. We say that a finite or infinite eigenvalue is *defective*, if one of the corresponding Jordan blocks in J or N is larger than one. By using the transformation matrices W and T, we can also write B and C as

$$B = W \begin{bmatrix} B_1 \\ B_2 \end{bmatrix}, \quad C = \begin{bmatrix} C_1 & C_2 \end{bmatrix} T,$$

to obtain an equivalent descriptor system.

Furthermore, we need some controllability and observability concepts [16]. The descriptor system (1.4) is called

- *completely controllable*, if $\operatorname{rank}\begin{bmatrix}\lambda E - A & B\end{bmatrix} = n$ for all $\lambda \in \mathbb{C}$ and furthermore $\operatorname{rank}\begin{bmatrix}E & B\end{bmatrix} = n$;
- *completely observable*, if $\operatorname{rank}\begin{bmatrix}\lambda E - A \\ C\end{bmatrix} = n$ for all $\lambda \in \mathbb{C}$ and furthermore $\operatorname{rank}\begin{bmatrix}E \\ C\end{bmatrix} = n$.

We can also define these concepts for single eigenvalues of $\lambda E - A$. A descriptor system (1.4) is called

- *controllable at* $\lambda \in \mathbb{C}$ if $\operatorname{rank}\begin{bmatrix}\lambda E - A & B\end{bmatrix} = n$;
- *controllable at* $\lambda = \infty$ if $\operatorname{rank}\begin{bmatrix}E & B\end{bmatrix} = n$;
- *observable* at $\lambda \in \mathbb{C}$ if $\operatorname{rank}\begin{bmatrix}\lambda E - A \\ C\end{bmatrix} = n$;
- *observable* at $\lambda = \infty$ if $\operatorname{rank}\begin{bmatrix}E \\ C\end{bmatrix} = n$;

otherwise it is called uncontrollable or unobservable at λ, respectively. Note that in the above definitions one can also consider each individual Jordan block of the Weierstraß canonical form separately in case of multiple eigenvalues. This is possible by considering the corresponding eigenvectors. Let x and y be right and left eigenvectors corresponding to a Jordan block in J or N of (2.1). Then

$$y^H \begin{bmatrix}\lambda E - A & B\end{bmatrix} = \begin{bmatrix}0 & y^H B\end{bmatrix}, \quad \begin{bmatrix}\lambda E - A \\ C\end{bmatrix} x = \begin{bmatrix}0 \\ Cx\end{bmatrix}.$$

We say that such a Jordan block is controllable if $B^T y \neq 0$, and observable if $Cx \neq 0$, otherwise we call it uncontrollable or unobservable. We use this definition when talking about controllability and observability of eigenvalues.

A descriptor system $\Sigma = (\lambda E - A, B, C)$ which induces the transfer function $G(s) = C(sE - A)^{-1}B$ is called a *realization* of $G(\cdot)$. Every rational function $G(\cdot)$ admits such a descriptor system realization. A realization of $G(\cdot)$ of the form (1.4) is called *minimal* if its order n is the smallest among all possible realizations. This is the case if and only if it is completely controllable and completely observable [16, Theorem 2-6.3].

The $\mathcal{H}_\infty$-norm has several applications, for instance it is used in model order reduction as an error measure. Assume that

$$\begin{aligned}\tilde{E}\dot{\tilde{x}}(t) &= \tilde{A}\tilde{x}(t) + \tilde{B}u(t),\\ \tilde{y}(t) &= \tilde{C}\tilde{x}(t),\end{aligned} \tag{2.2}$$

with $\tilde{E}$, $\tilde{A} \in \mathbb{R}^{r\times r}$, $\tilde{B} \in \mathbb{R}^{r\times m}$, $\tilde{C} \in \mathbb{R}^{p\times r}$, reduced descriptor vector $\tilde{x}(t) \in \mathbb{R}^r$ and output vector $\tilde{y}(t) \in \mathbb{R}^p$ is a stable reduced-order model of (1.4). Then the transfer function of the error system is given by

$$G_{\mathrm{err}}(s) = \begin{bmatrix}C & -\tilde{C}\end{bmatrix}\left(s\begin{bmatrix}E & 0\\ 0 & \tilde{E}\end{bmatrix} - \begin{bmatrix}A & 0\\ 0 & \tilde{A}\end{bmatrix}\right)^{-1}\begin{bmatrix}B\\ \tilde{B}\end{bmatrix}.$$

The value of $\|G_{\mathrm{err}}\|_{\mathcal{H}_\infty}$ can be interpreted as the worst-case error when evaluating $G_{\mathrm{err}}(\cdot)$ in the frequency domain.

Another field of application can be found in robust control where the $\mathcal{H}_\infty$-norm takes the role of a robustness measure. Consider a static output feedback controller $K \in \mathbb{R}^{m\times p}$ that stabilizes the system (1.4). This leads to the closed-loop dynamics

$$E\dot{x}(t) = A_K x(t) := (A + BKC)\, x(t).$$

In robust control we are interested in the robustness of the closed-loop systems with respect to perturbations in the controller K. In other words, we want to know how much we can maximally perturb K such that the perturbed closed-loop system

$$E\dot{x}(t) = A_{K+\Delta} x(t) = (A_K + B\Delta C)\, x(t)$$

is guaranteed to remain stable. To quantify robustness of a dynamical system, unstructured (i.e., for $B = C = I_n$) and structured stability radii were introduced, first by Hinrichsen and Pritchard in [28–30]. The generalization to matrix pencils is a nontrivial issue due to the fact that the influence of the infinite eigenvalues as well as perturbations that make the pencil singular have to be studied. For structured perturbations this has already been considered in [17]. In particular, it provides a relationship between the $\mathcal{H}_\infty$-norm and the structured complex stability radius. However, we have found an easier and more intuitive proof of this relation, outlined in Lemma 3.1 and Proposition 3.2. A further generalization of the structured complex stability radius has been analyzed in [19], allowing simultaneous structured perturbations of A and E. However, we do not consider perturbations of E since we would not have a relation to the $\mathcal{H}_\infty$-norm anymore. Another very good recent survey paper on robust stability of descriptor systems and stability radii of matrix pencils is [18].

For stable systems (1.4) we define the numbers

$$\begin{aligned} q^{\mathrm{f}}_{\mathbb{C}}(E,A,B,C) :&= \inf\left\{ \|\Delta\|_2 : \Lambda_{\mathrm{f}}(E, A+B\Delta C) \cap \mathrm{i}\mathbb{R} \neq \emptyset \text{ with } \Delta \in \mathbb{C}^{m\times p} \right\}, \\ q^{\infty}_{\mathbb{C}}(E,A,B,C) :&= \inf\big\{ \|\Delta\|_2 : \Lambda_\infty(E, A+B\Delta C) \text{ with } \Delta \in \mathbb{C}^{m\times p} \\ &\qquad \text{has controllable and observable defective eigenvalues or} \\ &\qquad \lambda E - (A+B\Delta C) \text{ is a singular pencil} \big\}, \end{aligned}$$

where $\Lambda_\infty(E,A)$ is the set of infinite eigenvalues of $\lambda E - A$ (counting multiplicities). Then we define the *structured complex stability radius of a matrix pencil* $\lambda E - A$ by

$$q_{\mathbb{C}}(E,A,B,C) := \min\left\{ q^{\mathrm{f}}_{\mathbb{C}}(E,A,B,C), q^{\infty}_{\mathbb{C}}(E,A,B,C) \right\}.$$

The value of $q^{\mathrm{f}}_{\mathbb{C}}(E,A,B,C)$ is the size of the smallest structured perturbation that makes the system unstable. The interpretation of $q^{\infty}_{\mathbb{C}}(E,A,B,C)$ is more involved. *Defective* infinite eigenvalues do not make the system unstable. However, if there are controllable and observable ones, we can construct an arbitrarily small structured perturbation such that the system will be unstable. This means that systems with controllable and observable defective infinite eigenvalues are on the "boundary to instability". If the perturbed matrix pencil becomes singular, then all complex numbers are eigenvalues and a part of the system dynamics is not well-defined.

It is desirable to make $q_{\mathbb{C}}(E,A,B,C)$ as large as possible in order to guarantee a very high robustness against perturbations in the controller. Later in this paper we show that for stable systems, it holds

$$q_{\mathbb{C}}(E,A,B,C) = \begin{cases} 1/\|G\|_{\mathcal{H}_\infty} & \text{if } G \not\equiv 0, \\ \infty & \text{if } G \equiv 0, \end{cases}$$

so a high value of $q_{\mathbb{C}}(E,A,B,C)$ corresponds to a small $\mathcal{H}_\infty$-norm of the transfer function $G(\cdot)$.

We also introduce the structured complex stability radius for a transfer function $G \in \mathcal{RH}_\infty^{p\times m}$ which slightly differs from the one for matrix pencils. For $\Delta \in \mathbb{C}^{m\times p}$ we define the perturbed transfer function

$$G_\Delta(s) := C\left(sE-(A+B\Delta C)\right)^{-1}B \tag{2.3}$$

and the numbers

$$\begin{aligned} r_{\mathbb{C}}^{\mathrm{f}}(E,A,B,C) :&= \inf\left\{\|\Delta\|_2 : \Pi_{\mathrm{f}}(E,A+B\Delta C,B,C)\cap \mathrm{i}\mathbb{R}\neq\emptyset \text{ with } \Delta\in\mathbb{C}^{m\times p}\right\},\\ r_{\mathbb{C}}^{\infty}(E,A,B,C) :&= \inf\{\|\Delta\|_2 : \Pi_\infty(E,A+B\Delta C,B,C)\neq\emptyset \text{ or } \lambda E-(A+B\Delta C)\\ &\qquad \text{is a singular pencil with } \Delta\in\mathbb{C}^{m\times p}\}\\ &= \inf\left\{\|\Delta\|_2 : G_\Delta(\cdot) \text{ as in (2.3) with } \Delta\in\mathbb{C}^{m\times p} \text{ is improper}\right.\\ &\qquad \left.\text{or not well-defined}\right\}, \end{aligned}$$

where $\Pi_\infty(E,A,B,C)$ is the set of infinite poles of $G(\cdot)$. Then the *structured complex stability radius of a transfer function* $G(\cdot)$ is defined by

$$r_{\mathbb{C}}(E,A,B,C) := \min\left\{r_{\mathbb{C}}^{\mathrm{f}}(E,A,B,C), r_{\mathbb{C}}^{\infty}(E,A,B,C)\right\}.$$

Remark 2.1. In fact, $r_{\mathbb{C}}(E,A,B,C)$ is the structured distance of a function $G\in\mathcal{RH}_\infty^{p\times m}$ to the set of functions which are not in $\mathcal{RH}_\infty^{p\times m}$, i.e.,

$$r_{\mathbb{C}}(E,A,B,C) = \inf\left\{\|\Delta\|_2 : G_\Delta \notin \mathcal{RH}_\infty^{p\times m} \text{ with } G_\Delta(\cdot) \text{ as in (2.3) and } \Delta\in\mathbb{C}^{m\times p}\right\}.$$

For stable or minimal descriptor systems, we have $q_{\mathbb{C}}^{\mathrm{f}}(E,A,B,C) = r_{\mathbb{C}}^{\mathrm{f}}(E,A,B,C)$ and $q_{\mathbb{C}}(E,A,B,C) = r_{\mathbb{C}}(E,A,B,C)$. However, $G\in\mathcal{RH}_\infty^{p\times m}$ can also be realized by an unstable descriptor system when all unstable eigenvalues are uncontrollable or unobservable. In this case, the definitions of $q_{\mathbb{C}}^{\mathrm{f}}(E,A,B,C)$ and $q_{\mathbb{C}}(E,A,B,C)$ do not make sense whereas those of $r_{\mathbb{C}}^{\mathrm{f}}(E,A,B,C)$ and $r_{\mathbb{C}}(E,A,B,C)$ do. It is very important to well distinguish between these definitions.

3. $\mathcal{H}_\infty$-Norm and Structured Stability Radius. In this subsection we prove an important relationship between the $\mathcal{H}_\infty$-norm and the structured complex stability radius.

LEMMA 3.1. *It holds that*

$$r_{\mathbb{C}}^{\infty}(E,A,B,C) = \begin{cases} 1/\lim\limits_{\omega\to\infty}\sigma_{\max}(G(\mathrm{i}\omega)) & \text{if } G\not\equiv 0,\\ \infty & \text{if } G\equiv 0. \end{cases}$$

Proof. If $G\equiv 0$, we cannot make the system improper by any structured perturbation, and therefore $r_{\mathbb{C}}^{\infty}(E,A,B,C)=\infty$. Consider the non-trivial case. W.l.o.g. we can assume that we have a minimal realization of a proper $G(\cdot)$ given in Weierstraß canonical form, i.e.,

$$\Sigma = \left(\lambda\begin{bmatrix} I_{n_{\mathrm{f}}} & 0\\ 0 & 0\end{bmatrix} - \begin{bmatrix} J & 0\\ 0 & I_{n_\infty}\end{bmatrix}, \begin{bmatrix} B_1\\ B_2\end{bmatrix}, \begin{bmatrix} C_1 & C_2\end{bmatrix}\right).$$

Note that for a minimal proper system, the nilpotent matrix N in the Weierstraß canonical form is zero or void. This follows from [16, Theorem 2-6.2 and Lemma

2-6.2]. Using this realization, it holds

$$\lim_{\omega\to\infty} G(\mathrm{i}\omega) = \begin{cases} -C_2B_2 & \text{if } N = 0, \\ 0 & \text{if } N \text{ is void.} \end{cases}$$

If N is void, then $r_{\mathbb{C}}^{\infty}(E, A, B, C) = \infty$. If $N = 0$, we consider structured perturbations of the matrix pencil which lead to

$$\begin{aligned} \lambda E_{\min} - A_{\min}^{\Delta} :&= \lambda \begin{bmatrix} I_{n_{\mathrm{f}}} & 0 \\ 0 & 0 \end{bmatrix} - \left(\begin{bmatrix} J & 0 \\ 0 & I_{n_\infty} \end{bmatrix} + \begin{bmatrix} B_1 \\ B_2 \end{bmatrix} \Delta \begin{bmatrix} C_1 & C_2 \end{bmatrix} \right) \\ &= \lambda \begin{bmatrix} I_{n_{\mathrm{f}}} & 0 \\ 0 & 0 \end{bmatrix} - \begin{bmatrix} J + B_1\Delta C_1 & B_1\Delta C_2 \\ B_2\Delta C_1 & I_{n_\infty} + B_2\Delta C_2 \end{bmatrix}, \end{aligned}$$

where $\Delta \in \mathbb{C}^{m\times p}$. Now we distinguish whether the pencil $\lambda E_{\min} - A_{\min}^{\Delta}$ is singular or not. If it is regular, then in [3, Theorem 3] it is shown that the perturbed transfer function is improper if and only if $I_{n_\infty} + B_2\Delta C_2$ is singular. If $\lambda E_{\min} - A_{\min}^{\Delta}$ is singular, then $\begin{bmatrix} B_2\Delta C_1 & I_{n_\infty} + B_2\Delta C_2 \end{bmatrix}$ contains linearly dependent rows. Hence, $I_{n_\infty} + B_2\Delta C_2$ is also singular in this case.

Therefore, we have to determine the value of

$$\begin{aligned} p_{\mathbb{C}} :&= \inf \left\{ \|\Delta\|_2 : I_{n_\infty} + B_2\Delta C_2 \text{ is singular with } \Delta \in \mathbb{C}^{m\times p} \right\} \\ &= \inf \left\{ \|\Delta\|_2 : -I_{n_\infty} + B_2\Delta C_2 \text{ is singular with } \Delta \in \mathbb{C}^{m\times p} \right\}. \end{aligned}$$

We consider the structured stability radius $r_{\mathbb{C}}(I_{n_\infty}, -I_{n_\infty}, B_2, C_2)$ of $-I_{n_\infty}$ with respect to B_2 and C_2. By employing [29, Proposition 2.1] we obtain

$$\begin{aligned} r_{\mathbb{C}}(I_{n_\infty}, -I_{n_\infty}, B_2, C_2) &= \frac{1}{\max\limits_{\omega\in\mathbb{R}} \sigma_{\max}(C_2((\mathrm{i}\omega + 1)I_{n_\infty})^{-1}B_2)} \\ &= \frac{1}{\sigma_{\max}(C_2B_2)} \\ &= \frac{1}{\lim\limits_{\omega\to\infty} \sigma_{\max}(G(\mathrm{i}\omega))}. \end{aligned} \tag{3.1}$$

Since the maximum in (3.1) is attained at $\omega = 0$, we have $p_{\mathbb{C}} = r_{\mathbb{C}}(I_{n_\infty}, -I_{n_\infty}, B_2, C_2)$. This shows the assertion. ∎

Proposition 3.2. *It holds*

$$r_{\mathbb{C}}(E, A, B, C) = \begin{cases} 1/\|G\|_{\mathcal{H}_\infty} & \text{if } G \not\equiv 0, \\ \infty & \text{if } G \equiv 0. \end{cases} \tag{3.2}$$

Proof. The proof is similar to the corresponding one for state-space systems in [29]. First we analyze the case that the value of the $\mathcal{H}_\infty$-norm is attained at some finite $\omega \in \mathbb{R}$.

Assume that for some $\Delta \in \mathbb{C}^{m\times p}$, $0 \neq x \in \mathbb{C}^m$, and $\omega \in \mathbb{R}$ we have

$$(A + B\Delta C)x = \mathrm{i}\omega Ex,$$

or equivalently

$$x = (\mathrm{i}\omega E - A)^{-1}B\Delta Cx.$$

Since $G(\cdot)$ is stable, we have $u := Cx \neq 0$, i.e.,

$$u = G(\mathrm{i}\omega)\Delta u. \tag{3.3}$$

If $G \equiv 0$ this leads to a contradiction and so $r^{\mathrm{f}}_{\mathbb{C}}(E, A, B, C) = \infty$, otherwise (3.3) implies $\|G(\mathrm{i}\omega)\|_2 \|\Delta\|_2 \geq 1$.

Now suppose that $\|G\|_{\mathcal{H}_\infty}$ is attained at ω_0, i.e., $\|G(\mathrm{i}\omega_0)\|_2 = \|G\|_{\mathcal{H}_\infty}$. Let

$$G(\mathrm{i}\omega_0) = \sum_{j=1}^{k} \sigma_j u_j v_j^H$$

be a singular value decomposition of $G(\mathrm{i}\omega_0)$ with $u_j \in \mathbb{C}^p$, $v_j \in \mathbb{C}^m$, $\|u_j\|_2 = \|v_j\|_2 = 1$, for $j = 1, \ldots, k := \min\{m, p\}$, and $\|G(\mathrm{i}\omega_0)\|_2 = \sigma_1 \geq \sigma_2 \geq \ldots \geq \sigma_k \geq 0$. With $\Delta := \sigma_1^{-1} v_1 u_1^H$ it follows that

$$G(\mathrm{i}\omega_0)\Delta u_1 = C(\mathrm{i}\omega_0 E - A)^{-1} B \Delta u_1 = u_1.$$

Defining $x := (\mathrm{i}\omega_0 E - A)^{-1} B \Delta u_1$ leads to $Cx = u_1$ and hence $x \neq 0$. This yields

$$x := (\mathrm{i}\omega_0 E - A)^{-1} B \Delta C x,$$

and consequently

$$(A + B\Delta C)\, x = \mathrm{i}\omega_0 E x.$$

From

$$x^H \begin{bmatrix} \mathrm{i}\omega_0 E^T - (A + B\Delta C)^T & C^T \end{bmatrix} = \begin{bmatrix} 0 & x^H C^T \end{bmatrix} = \begin{bmatrix} 0 & u_1 \end{bmatrix},$$

with $u_1 \neq 0$, we conclude that $\mathrm{i}\omega_0$ is an observable pole of the perturbed transfer function $G_\Delta(\cdot)$ as in (2.3). Similarly we can prove controllability of $\mathrm{i}\omega_0$.

From that we conclude $\|\Delta\|_2 = \frac{1}{\|G\|_{\mathcal{H}_\infty}}$, where Δ is a perturbation of infimal norm such that $\Pi_{\mathrm{f}}(E, A + B\Delta C, B, C) \cap \mathrm{i}\mathbb{R} \neq \emptyset$.

This shows that $\|G\|_{\mathcal{H}_\infty} = \|G(\mathrm{i}\omega)\|_2$ for some $\omega \in \mathbb{R}$ if and only if $r_{\mathbb{C}}(E, A, B, C) = r^{\mathrm{f}}_{\mathbb{C}}(E, A, B, C)$. The case that the norm value is attained at infinity is covered by Lemma 3.1. ∎

For the remainder of the article we need the following definitions.

Definition 3.3.

(a) The structured ε-pseudospectrum of the transfer function $G(\cdot)$ *with respect to B and C is defined by*

$$\Pi_\varepsilon(E, A, B, C) = \{s \in \mathbb{C} : s \in \Pi_{\mathrm{f}}(E, A + B\Delta C, B, C) \text{ for some } \Delta \in \mathbb{C}^{m\times p} \text{ with } \|\Delta\|_2 < \varepsilon\}.$$

(b) The structured ε-pseudospectrum of the transfer function $G(\cdot)$ is called regular *if there exists no $\Delta \in \mathbb{C}^{m\times p}$ with $\|\Delta\|_2 < \varepsilon$ such that $G_\Delta(\cdot)$ is improper or not well-defined.*

(c) The structured ε-pseudospectral abscissa *is given by*

$$\alpha_\varepsilon(E, A, B, C) := \max\{\operatorname{Re} s : s \in \Pi_\varepsilon(E, A, B, C)\}.$$

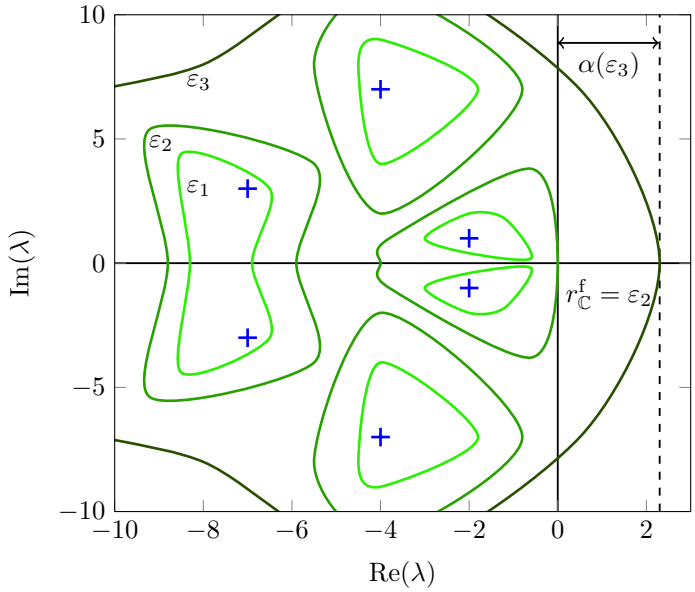

Fig. 3.1: Poles (blue crosses) and structured pseudospectra of a transfer function to different perturbation levels

The definition of regularity of a structured ε-pseudospectrum is strongly related to the so-called *admissibility* of perturbations [12, 18], i.e., a regular structured ε-pseudospectrum can only be generated by admissible perturbations. From the definition it is clear that regularity is equivalent to $\varepsilon < 1/\lim_{\omega\to\infty}\sigma_{\max}(G(\mathrm{i}\omega))$.

A graphical interpretation of the terms defined in Definition 3.3 is given in Figure 3.1.

It is also obvious that $\alpha_{r^{\mathrm{f}}_{\mathbb{C}}}(E, A, B, C) = 0$. So the main idea of our algorithm is to find the (unique) root of the function $\alpha(\varepsilon) := \alpha_\varepsilon(E, A, B, C)$. To get an efficient algorithm, we need to evaluate $\alpha(\varepsilon)$ for different values of ε in a cheap way. Then we can employ, e.g., Newton's method to compute the actual root.

4. Computation of the Structured ε-Pseudospectral Abscissa.

4.1. Derivation of the Basic Algorithm. In this subsection we derive a fast algorithm for computing $\alpha(\varepsilon)$. The following fundamental results are generalizations of the corresponding ones in [41].

LEMMA 4.1. *Let $s \in \mathbb{C}\backslash\Pi_{\mathrm{f}}(E, A, B, C)$ be given and $\varepsilon > 0$. Then the following statements are equivalent:*

(a) $s \in \Pi_\varepsilon(E, A, B, C)$.

(b) $\sigma_{\max}(G(s)) > \varepsilon^{-1}$.

(c) There exist vectors $u \in \mathbb{C}^m$ and $v \in \mathbb{C}^p$ with $\|u\|_2 < 1$ and $\|v\|_2 < 1$ such that $s \in \Pi_{\mathrm{f}}\left(E, A + \varepsilon B u v^H C, B, C\right)$, i.e., s is a pole of the perturbed transfer function $G_{\varepsilon u v^H}(\cdot)$.

Proof. "(a)$\Longrightarrow$(b)": From $s \in \Pi_\varepsilon(E, A, B, C)$ it follows that there exist a matrix $\Delta \in \mathbb{C}^{m\times p}$ with $\|\Delta\|_2 < \varepsilon$ and a vector $x \in \mathbb{C}^n$ such that

$$(sE - (A + B\Delta C))\, x = 0.$$

This is equivalent to

$$(sE - A)\, x = B\Delta Cx$$

and therefore

$$Cx = C\,(sE - A)^{-1}\, B\Delta Cx.$$

Now we can estimate

$$\|Cx\|_2 \leq \left\|C\,(sE - A)^{-1}\, B\right\|_2 \|\Delta\|_2 \,\|Cx\|_2\,,$$

and hence

$$\varepsilon^{-1} < \|\Delta\|_2^{-1} \leq \|G(s)\|_2\,.$$

"(b)$\Longrightarrow$(c)": Let $\sigma_{\max}(G(s)) > \varepsilon^{-1}$. Define $\sigma := \sigma_{\max}(G(s))$ with corresponding singular vectors $u \in \mathbb{C}^m$, $v \in \mathbb{C}^p$ satisfying $\|u\|_2 = \|v\|_2 = 1$. Then

$$G(s)u = \sigma v, \quad v^H G(s) = \sigma u^H, \quad \sigma > \varepsilon^{-1}. \tag{4.1}$$

Multiplying the first equation of (4.1) by v^H from the left and by $v^H C$ from the right yields

$$v^H C(sE - A)^{-1} B u v^H C = \sigma v^H v v^H C = \sigma v^H C.$$

By setting $y^H := v^H C(sE - A)^{-1}$ we obtain

$$y^H B u v^H C = \sigma y^H (sE - A).$$

It holds $y^H \neq 0$ since $v^H C \neq 0$, otherwise $\sigma = 0$ which is excluded since $\varepsilon > 0$. Therefore, $sE - \hat{A} := sE - \left(A + \sigma^{-1} B u v^H C\right)$ is singular. It remains to show that s is indeed a pole of the perturbed transfer function

$$C\left(sE - \hat{A}\right)^{-1} B,$$

i.e., we have to prove controllability and observability of s. Since y is a left eigenvector of $sE - \hat{A}$ it holds

$$y^H \begin{bmatrix} sE - \hat{A} & B \end{bmatrix} = \begin{bmatrix} 0 & y^H B \end{bmatrix} = \begin{bmatrix} 0 & v^H C(sE - A)^{-1} B \end{bmatrix} = \begin{bmatrix} 0 & \sigma u^H \end{bmatrix}.$$

Since $\sigma u^H \neq 0$, s is a controllable eigenvalue. Observability can be proven in an analogous manner and is therefore omitted. This yields statement (c) by noting that

$$\sigma^{-1} u v^H = \varepsilon \tilde{u} \tilde{v}^H \quad \text{with} \quad \tilde{u} = \sqrt{\varepsilon\sigma}u,\ \tilde{v} = \sqrt{\varepsilon\sigma}v,$$

where $\varepsilon\sigma < 1$ by definition.

"(c)$\Longrightarrow$(a)": This statement is trivial since with $\Delta := \varepsilon u v^H$ we obtain $s \in \Pi_{\mathrm{f}}(E, A + B\Delta C, B, C)$. ∎

By employing the same techniques as in the proof of the previous lemma we can also show the following result.

COROLLARY 4.2. *Let $\varepsilon > 0$ and $s \in \mathbb{C}\backslash\Pi_{\mathrm{f}}(E, A, B, C)$. Then the following statements are equivalent:*

(a) $G(s)$ *has a (not necessarily maximum) singular value* ε^{-1} *with right and left singular vectors* u *and* v *satisfying* $\|u\|_2 = \|v\|_2 = 1$.

(b) The number s *is a controllable and observable eigenvalue of the perturbed pencil* $\lambda E - (A + \varepsilon B u v^H C)$ *with associated right and left eigenvectors* x *and* y *given by*

$$x = (sE - A)^{-1} B u, \quad \text{and} \quad y = (sE - A)^{-H} C^T v. \tag{4.2}$$

From Lemma 4.1 we can conclude that

$$\Pi_\varepsilon(E, A, B, C) = \Pi_{\mathrm{f}}(E, A, B, C) \cup \left\{ s \in \mathbb{C} : \sigma_{\max}\left(G(s)\right) > \varepsilon^{-1} \right\}$$

with boundary

$$\partial\Pi_\varepsilon(E, A, B, C) = \left\{ s \in \mathbb{C} : \sigma_{\max}\left(G(s)\right) = \varepsilon^{-1} \right\}. \tag{4.3}$$

In other words, also the rightmost structured pseudopole is arbitrarily close to the curve $\partial\Pi_\varepsilon(E, A, B, C)$. Thus, our strategy consists of computing a sequence of suitable structured rank-1 perturbed pencils $\lambda E - (A + \varepsilon B u v^H C)$ such that one of the perturbed eigenvalues converges to the rightmost structured pseudopole of $G(\cdot)$. A similar technique has already been successfully applied to compute the pseudospectral abscissa of a matrix, see [26]. For computational purposes we assume that ε is chosen such that the corresponding structured ε-pseudospectrum is regular. In this way we guarantee that we only consider admissible perturbations of *finite* eigenvalues and that $\alpha(\varepsilon)$ is *finite*. Inadmissible perturbations are covered by evaluating $\lim_{\omega\to\infty} \sigma_{\max} G(\mathrm{i}\omega)$ which will be done separately.

We need the following result for the first order perturbation theory of matrix pencils. By $\mathbb{C}[\lambda]^{n\times n}$ we denote the set of all polynomials in λ with coefficients in $\mathbb{C}^{n\times n}$.

LEMMA 4.3. *[46] Let* $\lambda E - A \in \mathbb{C}[\lambda]^{n\times n}$ *be a given regular matrix pencil and let* x, $y \in \mathbb{C}^n$ *be right and left eigenvectors corresponding to a simple finite eigenvalue* $\lambda = \frac{y^H A x}{y^H E x}$. *Let* $\lambda E - (A + t B u v^H C)$ *be a perturbed regular matrix pencil with eigenvalue* $\tilde{\lambda}$. *Then it holds*

$$\tilde{\lambda} = \lambda + t \frac{y^H B u v^H C x}{y^H E x} + \mathcal{O}\left(t^2\right).$$

Furthermore, Lemma 4.3 directly yields

$$\left.\frac{\mathrm{d}\tilde{\lambda}(t)}{\mathrm{d}t}\right|_{t=0} = \frac{y^H B u v^H C x}{y^H E x}.$$

Now, we describe how such rank-1 perturbations can be constructed in an optimal way. Therefore, let λ be a simple eigenvalue of the pencil $\lambda E - A$ with corresponding right and left eigenvectors x, y satisfying $y^H E x > 0$. Furthermore, let $u \in \mathbb{C}^m$ and $v \in \mathbb{C}^p$ with $\|u\|_2 = \|v\|_2 = 1$ be given vectors. Then, it holds

$$\begin{aligned} \operatorname{Re}\left(\left.\frac{\mathrm{d}\tilde{\lambda}(t)}{\mathrm{d}t}\right|_{t=0} \right) &= \frac{\operatorname{Re}\left(y^H B u v^H C x\right)}{y^H E x} \\ &\leq \frac{\left\|y^H B\right\|_2 \|C x\|_2}{y^H E x}. \end{aligned} \tag{4.4}$$

Equality in (4.4) holds for $u = B^T y/\left\|B^T y\right\|_2$, $v = Cx/\|Cx\|_2$. Hence, local maximal growth in $\mathrm{Re}\left(\tilde{\lambda}(t)\right)$ as t increases from 0 is achieved for this choice of u and v. In this way we generate the initial perturbation. Next we consider subsequent perturbations. Let therefore $\lambda E - \hat{A} := \lambda E - (A + \varepsilon B\hat{u}\hat{v}^H C)$ with a simple eigenvalue $\hat{\lambda}$ and associated right and left eigenvectors $\hat{x}$, $\hat{y}$ with $\hat{y}^H E\hat{x} > 0$ be the perturbed matrix pencil. In addition let vectors $u \in \mathbb{C}^m$, $v \in \mathbb{C}^p$ with $\|u\|_2 = \|v\|_2 = 1$ be given. We consider the family of perturbations of the matrix pencil $\lambda E - \hat{A}$ of the form

$$\lambda E - \left(\hat{A} + tB\left(uv^H - \hat{u}\hat{v}^H\right)C\right),$$

which are structured ε-norm rank-1 perturbations of $\lambda E - A$ for $t = 0$ and $t = \varepsilon$. For the perturbed eigenvalue, for simplicity called again $\tilde{\lambda}$, we obtain

$$\begin{aligned}\mathrm{Re}\left(\left.\frac{\mathrm{d}\tilde{\lambda}(t)}{\mathrm{d}t}\right|_{t=0}\right) &= \frac{\mathrm{Re}\left(\hat{y}^H B\left(uv^H - \hat{u}\hat{v}^H\right)C\hat{x}\right)}{\hat{y}^H E\hat{x}} \\ &\leq \frac{\left\|\hat{y}^H B\right\|_2 \|C\hat{x}\|_2 - \mathrm{Re}\left(\hat{y}^H B\hat{u}\hat{v}^H C\hat{x}\right)}{\hat{y}^H E\hat{x}}. \end{aligned} \tag{4.5}$$

Similarly to the above considerations, equality in (4.5) holds for $u = B^T\hat{y}/\left\|B^T\hat{y}\right\|_2$, $v = C\hat{x}/\|C\hat{x}\|_2$. So, the basic algorithm consists of successively choosing an eigenvalue and constructing the perturbations described above by using the corresponding eigenvectors. However, an important question is how to actually choose these eigenvalues. This will be discussed in the next subsection.

4.2. Choice of the Eigenvalues. Recall that we want to construct structured ε-norm rank-1 perturbations of the pencil $\lambda E - A$ such that one of the perturbed eigenvalues converges to the rightmost pseudopole of the corresponding transfer function $G(\cdot)$. Intuitively, in each step one would choose the rightmost eigenvalue of the perturbed pencil to construct the next perturbation. However, that might not be a good choice. Note that the perturbability of an eigenvalue λ with right and left normalized eigenvectors x and y highly depends on $\left\|B^T y\right\|_2$ and $\|Cx\|_2$. If these values are small, no large perturbation is possible. We recall that these values are strongly related to the controllability and observability concepts introduced in Section 1. Roughly speaking, the "larger" $\left\|B^T y\right\|_2$ is, the "larger" is the distance of the system to uncontrollability at λ. So, large values of $\left\|B^T y\right\|_2$ indicate a good controllability at λ. Similar considerations can also be made for observability.

Consequently, for our algorithm we look for eigenvalues that have both sufficiently large real part and a high controllability and observability. An algorithm which unites both concepts is the *(subspace accelerated MIMO) dominant pole algorithm (SAMDP)*, introduced by Rommes and Martins [42–45]. This algorithm can be shown to locally superlinearly converge to the desired eigenvalues. It has actually been designed to find the poles which have the highest influence on the frequency response of the transfer function $G(\cdot)$. Assume that $\lambda E - A$ has only simple eigenvalues λ_k with left and right eigenvectors y_k and x_k, normalized such that $y_k^H E x_k = 1$. Then

$$G(s) = \sum_{k=1}^{n} \frac{R_k}{s - \lambda_k} + R_\infty \tag{4.6}$$

with the *residues*

$$R_k = Cx_k y_k^H B \quad \text{and} \quad R_\infty = \lim_{\omega\to\infty} G(\mathrm{i}\omega).$$

Then,

$$\|R_k\|_2 = \lambda_{\max}\left(Cx_k y_k^H BB^T y_k x_k^H C^T\right)^{1/2} = \|Cx_k\|_2 \left\|B^T y_k\right\|_2$$

is a measure for simultaneous controllability and observability of λ_k. We observe that if λ_j is close to the imaginary axis and $\|R_j\|_2$ is large, then for $\omega \approx \mathrm{Im}(\lambda_j)$ it holds

$$G(\mathrm{i}\omega) \approx \frac{R_j}{-\mathrm{Re}(\lambda_j)} + \sum_{\substack{k=1\\k\neq j}}^{n} \frac{R_k}{\mathrm{i}\omega - \lambda_k} + R_\infty,$$

and therefore, $\|G(\mathrm{i}\omega)\|_2$ is large, too. These considerations give the motivation for the following definition. We call an eigenvalue $\lambda_j \in \Lambda(E,A)$ *dominant pole* of $G(\cdot)$, if

$$\frac{\|R_k\|_2}{|\mathrm{Re}(\lambda_k)|} < \frac{\|R_j\|_2}{|\mathrm{Re}(\lambda_j)|}, \quad k = 1, \ldots, n, \quad k \neq j. \tag{4.7}$$

The most dominant poles can be determined by SAMDP and are essentially what we are looking for. However, we also deal with positive structured pseudospectral abscissae. By using the definition (4.7), the eigenvalues tend to loose dominance as soon as they have crossed the imaginary axis into the right half-plane. Then, in subsequent iterations eigenvalues in the left half-plane tend to be determined as most dominant. This is of course an undesired behavior since this could lead to convergence problems when the rightmost pseudoeigenvalue is "far" in the right half-plane. Therefore, we also propose an alternative dominance measure which does not have this drawback. We call an eigenvalue $\lambda_j \in \Lambda_{\mathrm{f}}(E,A)$ *exponentially dominant pole* of $G(\cdot)$, if

$$\|R_k\|_2 \exp(\beta\,\mathrm{Re}(\lambda_k)) \;<\; \|R_j\|_2 \exp(\beta\,\mathrm{Re}(\lambda_j)), \quad k \;=\; 1, \ldots, n, \quad k \;\neq\; j. \tag{4.8}$$

The parameter β is a weighting factor which defines the trade-off between the influence of the residue and real part of the eigenvalues. In our numerical experiments it turned out that dominance defined by (4.7) or (4.8) with rather large values of β (high weight on the real part) are good choices for many examples. Since SAMDP delivers the poles which have the highest influence on the frequency response of a system and due to the relation (3.2), we can determine very good initial estimates for $r_{\mathbb{C}}^{\mathrm{f}}(E,A,B,C)$. We compute some of the dominant poles λ_k, $k = 1, \ldots, \ell$ and determine an estimate $r_{\mathbb{C}}^{\mathrm{est}}(E,A,B,C)$ as

$$r_{\mathbb{C}}^{\mathrm{est}}(E,A,B,C) = 1/\max_{1\leq k\leq \ell} \sigma_{\max}\left(G\left(\mathrm{i}\omega_k\right)\right) \tag{4.9}$$

with $\omega_k = \mathrm{Im}(\lambda_k)$, $k = 1, \ldots, \ell$.

4.3. Algorithmic Details. In this subsection we present some pseudocode of the algorithms that have been derived. Algorithm 1 summarizes the procedure for the computation of the structured ε-pseudospectral abscissa. In our implementation we always initialize Algorithm 1 by setting x_0 and y_0 to the eigenvectors returned by the previous $\alpha(\varepsilon)$-evaluation (if there is one). This accelerates the computation drastically since the eigenvectors converge as well in the final root-finding steps.

We mention the drawback that the algorithm not necessarily converges to the globally rightmost value on the boundary of the ε-pseudospectrum $\partial\Pi_\varepsilon(E,A,B,C)$

Algorithm 1 Computation of the structured pseudospectral abscissa

Input: System $\Sigma = (\lambda E - A, B, C)$, perturbation level $\varepsilon < 1/\lim_{\omega\to\infty} \sigma_{\max}(G(\mathrm{i}\omega))$, tolerance on relative change τ, dominance measure as in (4.7) or (4.8) for all dominant pole computations.

Output: $\alpha_\varepsilon(E, A, B, C)$, right and left eigenvectors x_* and y_* associated to the optimal pseudopole.

1: Compute the dominant pole λ_0 of $(\lambda E - A, B, C)$ with left and right eigenvectors y_0 and x_0.
2: Compute the perturbation $\hat{A} = A + \varepsilon \frac{BB^T y_0 x_0^H C^T C}{\|B^T y_0\|_2 \|C x_0\|_2}$.
3: **for** $j = 1, 2, \ldots$ **do**
4: Compute the dominant pole λ_j of $(\lambda E - \hat{A}, B, C)$ with left and right eigenvectors y_j and x_j.
5: **if** $|\mathrm{Re}\,(\lambda_j) - \mathrm{Re}\,(\lambda_{j-1})| < \tau\,|\mathrm{Re}\,(\lambda_j)|$ **then**
6: Set $k = j$.
7: Break.
8: **end if**
9: Compute the perturbation $\hat{A} = A + \varepsilon \frac{BB^T y_j x_j^H C^T C}{\|B^T y_j\|_2 \|C x_j\|_2}$.
10: **end for**
11: Set $\alpha_\varepsilon(E, A, B, C) = \mathrm{Re}\,(\lambda_k)$, $x_* = x_k$, $y_* = y_k$.

in (4.3). Mostly it does but in some rare situations the algorithm converges only to a local maximizer. This especially happens in the first iteration of the root-finding algorithm when no good estimates of the optimal eigenvectors are available. Therefore, sometimes one has to try several dominant poles to find the global maximizer in the beginning. Note that we could also follow multiple poles to the boundary of the corresponding pseudospectrum in order to increase the chance to find the globally rightmost point. But due to the much higher complexity and a comparably small gain we only follow one pole. In fact, by choosing the dominant pole of the original transfer function as starting pole usually gives the desired result as shown in Section 7.

4.4. Fixed Point Analysis. This section is devoted to the analysis of the fixed points of the iteration given by Algorithm 1. The following two lemmas will be needed in our considerations

LEMMA 4.4. *[26] Let $t \in \mathbb{R}$ and consider the $p \times m$ matrix family $C(t) = C_0 + tC_1$. Let $\sigma(t)$ be a singular value of $C(t)$ converging to a simple nonzero singular value σ_0 of C_0 as $t \to 0$. Then, $\sigma(t)$ is analytic near $t = 0$ and*

$$\left.\frac{\mathrm{d}\sigma(t)}{\mathrm{d}t}\right|_{t=0} = v_0^H C_1 u_0,$$

where u_0 and v_0 with $\|u_0\|_2 = \|v_0\|_2 = 1$ are, respectively, the right and left singular vectors of C_0 corresponding to σ_0.

LEMMA 4.5. *[36] Let $s_* \in \mathbb{C}$ be not a pole of the transfer function $G(\cdot)$. Then, $G(\cdot)$ can be expanded into a Laurent series at s_* as*

$$\begin{aligned} G(s) &= C\big(I_n - \big(s - s_*\big)(s_*E - A)^{-1}E\big)^{-1}(s_*E - A)^{-1}B \\ &= M_0 + M_1(s - s_*) + M_2(s - s_*)^2 + \ldots \end{aligned}$$

with the moments $M_j = -C\left((s_*E - A)^{-1}E\right)^j (s_*E - A)^{-1}B$.

Besides the above we will make the following assumption [22, Assumption 2.19] throughout this section.

ASSUMPTION 4.6. *Let $\varepsilon > 0$ be given such that the associated structured ε-pseudospectrum is regular. Let $s_* \in \mathbb{C}$ be a locally rightmost point of $\Pi_\varepsilon(E, A, B, C)$. Then we assume that*

(a) the largest singular value ε^{-1} of $G(s_*)$ is simple;

(b) if u_* and v_* are the corresponding right and left singular vectors with $\|u_*\|_2 = \|v_*\|_2 = 1$, then the pole s_* of the perturbed transfer function $G_{\varepsilon u_* v_*^H}(\cdot)$ is simple. (That s_* is a pole follows from Corollary 4.2.)

Note, that using similar arguments as in [10, p. 362], the first part of Assumption 4.6 is generically true, i.e., it holds for almost all systems $\Sigma = (\lambda E - A, B, C)$. However, it is not difficult to find counter-examples.

LEMMA 4.7. *Let Assumption 4.6 be satisfied. If $s_* \in \mathbb{C}$ is a local maximizer of the optimization problem*

$$\max\left\{\mathrm{Re}(s) : s \in \Pi_\varepsilon(E, A, B, C)\right\}, \tag{4.10}$$

then

$$\|G(s_*)\|_2 = \varepsilon^{-1} \quad \text{and} \quad v_*^H C\left(s_*E - A\right)^{-1} E\left(s_*E - A\right)^{-1} Bu_* > 0,$$

where u_* and v_* are the normalized right and left singular vectors of $G(s_*)$.

Proof. Our proof follows similar arguments as in the proof of [22, Lemma 2.21]. The assertion that $\|G(s_*)\|_2 = \varepsilon^{-1}$ directly follows from the fact that s_* is on the boundary of $\Pi_\varepsilon(E, A, B, C)$. Next, the optimization problem (4.10) is equivalent to

$$\max\left\{\mathrm{Re}(s) : \|G(s)\|_2 \geq \varepsilon^{-1}\right\}.$$

By identifying $s = \gamma + \mathrm{i}\delta \in \mathbb{C}$ with the vector $\left[\begin{smallmatrix}\gamma\\ \delta\end{smallmatrix}\right] \in \mathbb{R}^2$, this is furthermore equivalent to

$$\max\left\{g(\gamma, \delta) : h(\gamma, \delta) \leq 0\right\}$$

with $g(\gamma, \delta) = \gamma$ and $h(\gamma, \delta) = \varepsilon^{-1} - \|G(\gamma + \mathrm{i}\delta)\|_2$. At the optimum $\left[\begin{smallmatrix}\gamma_*\\ \delta_*\end{smallmatrix}\right]$ we must now either have

(i) $\nabla h(\gamma_*, \delta_*) = 0$; or

(ii) $\nabla g(\gamma_*, \delta_*) = \mu \nabla h(\gamma_*, \delta_*)$ with a Lagrange multiplier $\mu > 0$.

From Lemma 4.5 it follows that in a neighborhood of $s_* = \gamma_* + \mathrm{i}\delta_*$ we have

$$G(s) = -C(s_*E - A)^{-1}B + (s_* - s)C(s_*E - A)^{-1}E(s_*E - A)^{-1}B + \mathcal{O}\left((s_* - s)^2\right).$$

By applying Lemma 4.4 to $G(\cdot)$, we obtain

$$\nabla h(\gamma_*, \delta_*) = \begin{bmatrix} \mathrm{Re}\left(v_*^H C\left(s_*E - A\right)^{-1} E\left(s_*E - A\right)^{-1} Bu_*\right) \\ \mathrm{Im}\left(v_*^H C\left(s_*E - A\right)^{-1} E\left(s_*E - A\right)^{-1} Bu_*\right) \end{bmatrix}.$$

Since s_* is an eigenvalue of the pencil $\lambda E - (A + \varepsilon Bu_* v_*^H C)$ with right and left eigenvectors x_* and y_* we obtain

$$\begin{aligned} x_* &= \varepsilon(s_*E - A)^{-1}Bu_*v_*^H Cx_*, \\ y_*^H &= \varepsilon y_*^H Bu_*v_*^H C(s_*E - A)^{-1}, \end{aligned}$$

and hence

$$0 \neq y_*^H E x_* = \varepsilon^2 y_*^H B u_* v_*^H C (s_* E - A)^{-1} E (s_* E - A)^{-1} B u_* v_*^H C x_*.$$

This means that $v_*^H C (s_* E - A)^{-1} E (s_* E - A)^{-1} B u_* \neq 0$ and as a consequence we can exclude case (i) above. Since $\nabla g(\gamma_*, \delta_*) = \left[\begin{smallmatrix} 1 \\ 0 \end{smallmatrix}\right]$ and (ii) holds, we directly obtain

$$v_*^H C \left(s_* E - A\right)^{-1} E \left(s_* E - A\right)^{-1} B u_* = 1/\mu > 0$$

and the proof is complete. ∎

Lemma 4.7 gives necessary first-order optimality conditions for $s_* \in \mathbb{C}$ to be a locally rightmost point in the structured ε-pseudospectrum. Now we can start analyzing the fixed points of the iteration presented in Algorithm 1. First we introduce the notion of a fixed point similar as in [22, Definition 3.1]. Here, the term "dominant pole" is either understood with respect to (4.7) or (4.8).

Definition 4.8. *Let $\varepsilon > 0$ such that the associated structured ε-pseudospectrum is regular. Let furthermore $((u_j, v_j))_{j=0}^{\infty} = \left(\left(B^T y_j / \left\|B^T y_j\right\|_2, C x_j / \left\|C x_j\right\|_2\right)\right)_{j=0}^{\infty}$ be a sequence of perturbations constructed by Algorithm 1 and let s_j denote the dominant pole of the perturbed transfer function $G_{\varepsilon u_j v_j^H}(\cdot)$. A vector pair (u_j, v_j) is a* fixed point *of this iteration if s_j is simple, $u_j v_j^H = u_{j+1} v_{j+1}^H$, and consequently $s_j = s_{j+1}$.*

Next, we get a similar theorem as [22, Theorem 3.2] which we will prove in an analogous fashion.

Theorem 4.9.

(a) Let $\varepsilon > 0$ be chosen such that the corresponding structured ε-pseudospectrum is regular. Let (u_*, v_*) be a fixed point of the iteration induced by Algorithm 1 corresponding to the dominant pole s_* of $G_{\varepsilon u_* v_*^H}(\cdot)$. Then $G(s_*)$ has a singular value equal to ε^{-1} and if this is the largest one, the first-order optimality conditions presented in Lemma 4.7 hold.

(b) Conversely, assume that $\varepsilon > 0$ be chosen such that the corresponding structured ε-pseudospectrum is regular and that the first-order optimality conditions in Lemma 4.7 hold true for some s_* and (u_*, v_*). Then s_* is a pole of $G_{\varepsilon u_* v_*^H}(\cdot)$ and if it is the dominant one and simple, then (u_*, v_*) is a fixed point of the iteration induced by Algorithm 1.

Proof.

(a) Let (u_*, v_*) be a fixed point of the iteration induced by Algorithm 1 corresponding the dominant pole s_* of $G_{\varepsilon u_* v_*^H}(\cdot)$. Then $u_* = B^T y_* / \left\|B^T y_*\right\|_2$ and $v_* = C x_* / \left\|C x_*\right\|_2$, where x_* and y_* are the right and left eigenvectors of the perturbed matrix pencil

$$\lambda E - \left(A + \varepsilon \frac{B B^T y_* x_*^H C^T C}{\left\|B^T y_*\right\|_2 \left\|C x_*\right\|_2}\right) \tag{4.11}$$

to the eigenvalue s_*. That ε^{-1} is indeed a singular value of $G(s_*)$ follows by Corollary 4.2. Let ε^{-1} now be the largest singular value of $G(s_*)$. Then we have

$$x_* = \varepsilon \frac{(s_* E - A)^{-1} B B^T y_* x_*^H C^T C x_*}{\left\|B^T y_*\right\|_2 \left\|C x_*\right\|_2},$$
$$y_*^H = \varepsilon \frac{y_*^H B B^T y_* x_*^H C^T C (s_* E - A)^{-1}}{\left\|B^T y_*\right\|_2 \left\|C x_*\right\|_2}.$$

Due to the normalization $y_*^H E x_* = 1$ we now obtain

$$\begin{aligned} y_*^H E x_* &= \varepsilon^2 \left\|B^T y_*\right\|_2 \|C x_*\|_2 \frac{x_*^H C^T}{\|C x_*\|_2} C \left(s_* E - A\right)^{-1} E \left(s_* E - A\right)^{-1} B \frac{B^T y_*}{\|B^T y_*\|_2} \\ &= 1 > 0, \end{aligned} \tag{4.12}$$

i.e., the first-order optimality condition holds true.

(b) Now assume that the first-order optimality conditions in Lemma 4.7 are satisfied for some s_* and (u_*, v_*). Then $\sigma_{\max}\left(G(s_*)\right) = \varepsilon^{-1}$ with right and left normalized singular vectors $u_* = B^T y_* / \left\|B^T y_*\right\|_2$ and $v_* = C x_* / \|C x_*\|_2$. From the second optimality condition in Lemma 4.7 and with (4.2) we obtain

$$\frac{x_*^H C^T C (s_* E - A)^{-1} E (s_* E - A)^{-1} B B^T y_*}{\|C x_*\|_2 \|B^T y_*\|_2} > 0,$$

where x_* and y_* are now again the right and left eigenvectors of the perturbed pencil (4.11) to the eigenvalue s_*. So, if s_* is dominant and simple, then the pair (u_*, v_*) is a fixed point of the iteration.

□

Similarly as in [26, p. 1176] we argue that the only possible *attractive* fixed points of the iteration given by Algorithm 1 are the local maximizers of the optimization problem (4.10).

4.5. Local Convergence and Error Analysis. Similarly as in [26] it is possible to show that for sufficiently small values of ε we have local convergence to a fixed point with linear rate. The generalization of the proof is analogous to the one for the algorithm in [22], as discussed by [25]. Due to space constraints we omit the details. However, as shown by our numerical examples we always have convergence to a fixed point independently from ε. However, similarly as in [26], the linear convergence factor might get higher for larger values of ε.

5. Newton's Method for Computing the Structured Stability Radius. In this section we derive a Newton-like method for computing the root of $\alpha(\varepsilon)$. This is a generalization of the method presented in [22] and we will later show that it is slightly faster than the secant method used in [6] or any other superlinearly converging root-finding scheme [5] applied to this problem. The following theorem deals with the derivative of the structured pseudospectral abscissa with respect to ε, similarly as in [22, Theorem 4.1].

THEOREM 5.1. *Let $\varepsilon > 0$ be chosen such that the associated structured ε-pseudospectrum is regular. Let $s(\varepsilon)$ be the rightmost point of $\Pi_\varepsilon(E, A, B, C)$. Assume that Assumption 4.6 holds for all regular structured ε-pseudospectra and let $u(\varepsilon) = B^T y(\varepsilon) / \left\|B^T y(\varepsilon)\right\|_2$ and $v(\varepsilon) = C x(\varepsilon) / \|C x(\varepsilon)\|_2$ be the normalized singular vectors of $G(s(\varepsilon))$ corresponding to the largest singular value ε^{-1}, where $x(\varepsilon)$ and $y(\varepsilon)$ are the right and left eigenvectors of the perturbed pencil*

$$\lambda E - \left(A + \varepsilon \frac{B B^T y(\varepsilon) x(\varepsilon)^H C^T C}{\|B^T y(\varepsilon)\|_2 \|C x(\varepsilon)\|_2}\right),$$

with $y(\varepsilon)^H E x(\varepsilon) = 1$. Furthermore, let $\varepsilon_0 > 0$ be given such that the structured ε_0-pseudospectrum is regular and such that the rightmost point $s(\varepsilon_0)$ of $\Pi_{\varepsilon_0}(E, A, B, C)$

is uniquely determined. Then, $s(\varepsilon)$ is continuously differentiable at ε_0 and it holds that

$$\left.\frac{\mathrm{d}\alpha(\varepsilon)}{\mathrm{d}\varepsilon}\right|_{\varepsilon=\varepsilon_0} = \left.\frac{\mathrm{d}s(\varepsilon)}{\mathrm{d}\varepsilon}\right|_{\varepsilon=\varepsilon_0} = \left\|B^T y(\varepsilon_0)\right\|_2 \left\|Cx(\varepsilon_0)\right\|_2 . \tag{5.1}$$

Proof. The proof is similar as for [22, Theorem 4.1]. Due to the first part of Assumption 4.6, the singular vectors $u(\varepsilon)$ and $v(\varepsilon)$ are unique up to multiplication with a unitary scalar. Therefore, the largest singular value of $G(s(\varepsilon))$ is differentiable with respect to ε. The second part of Assumption 4.6 ensures that $y(\varepsilon)^H E x(\varepsilon) \neq 0$ while the uniqueness of the rightmost point $s(\varepsilon_0)$ guarantees the continuity of $s(\varepsilon)$ and its derivative in a neighborhood of ε_0.

Now we prove (5.1). Differentiating the constraint $G(s(\varepsilon)) = \varepsilon^{-1}$ with respect to ε yields

$$\begin{aligned} 0 &= \frac{\mathrm{d}}{\mathrm{d}\varepsilon}\left(\varepsilon^{-1} - \left\|C(s(\varepsilon)E - A)^{-1}B\right\|_2\right) \\ &= -\varepsilon^{-2} + v(\varepsilon)^H C\left(s(\varepsilon)E - A\right)^{-1} E\left(s(\varepsilon)E - A\right)^{-1} B u(\varepsilon) \cdot \frac{\mathrm{d}s(\varepsilon)}{\mathrm{d}\varepsilon}. \end{aligned}$$

Plugging in $u(\varepsilon) = B^T y(\varepsilon) / \left\|B^T y(\varepsilon)\right\|_2$ and $v(\varepsilon) = Cx(\varepsilon) / \left\|Cx(\varepsilon)\right\|_2$ and comparing this with (4.12) gives the desired result and finalizes the proof. ∎

Now, since we know how to differentiate $\alpha(\varepsilon)$, we can make use of Newton's method to compute the root of $\alpha(\cdot)$. This method has a local quadratic convergence since $\mathrm{d}\alpha(\varepsilon)/\mathrm{d}\varepsilon > 0$ and $\mathrm{d}^2\alpha(\varepsilon)/\mathrm{d}\varepsilon^2$ is finite. The complete procedure is summarized in Algorithm 2. First, we check whether the $\mathcal{H}_\infty$-norm is attained at $\omega = \infty$. This is done by evaluating $\sigma_{\max}(G(\cdot))$ at the imaginary parts of the dominant poles. If all these values are below $g_\infty := \lim_{\omega\to\infty} \sigma_{\max}\left(G(\mathrm{i}\omega)\right)$, we assume that the norm is attained at infinity and we return g_∞. This step is necessary to avoid possible computations with nonregular structured pseudospectra in subsequent steps. To estimate $\lim_{\omega\to\infty} G(\mathrm{i}\omega)$, we evaluate $G(\mathrm{i}\omega)$ for a sufficiently large ω. The largest singular value of $G(\mathrm{i}\omega)$ will converge quickly due to the fact that for large ω there are no close finite poles which can introduce peaks. We can give the following upper bound using the residue representation of the transfer function (4.6) with $\lambda_j = \nu_j + \mathrm{i}\omega_j$, $j = 1, \ldots, n$:

$$\begin{aligned} \left\|G(\mathrm{i}\omega)\right\|_2 &= \left\|\sum_{j=1}^{n} \frac{R_j}{\mathrm{i}\omega - \mathrm{i}\omega_j - \nu_j} + R_\infty\right\|_2 \\ &\leq \sum_{j=1}^{n} \frac{\left\|R_j\right\|_2}{\left|\mathrm{i}\omega - \mathrm{i}\omega_j - \nu_j\right|} + \left\|R_\infty\right\|_2 . \end{aligned} \tag{5.2}$$

For $\omega \gg \max_{1\leq j\leq n} \omega_j$ we can neglect the real parts of the denominators ν_j, $j = 1, \ldots, n$. Since usually there are only very few dominant poles, we can control the desired accuracy by, e.g., choosing ω such that for the most dominant poles λ_j, $j = 1, \ldots, \ell$, we have

$$\sum_{j=1}^{\ell} \frac{\left\|R_j\right\|_2}{\left|\omega - \omega_j\right|} \leq \eta \tag{5.3}$$

for some small $\eta > 0$. Note that in the algorithm, the dominant poles have to be computed anyway, so we can evaluate the left-hand side of (5.3) at no additional cost.

Algorithm 2 Computation of the $\mathcal{H}_\infty$-norm

Input: System $\Sigma = (\lambda E - A, B, C)$ with transfer function $G(\cdot)$.
Output: $\|G\|_{\mathcal{H}_\infty}$, optimal frequency ω_*.

```
Compute some dominant poles λ_j = ν_j + iω_j, j = 1, ..., ℓ.
Compute g_∞ := lim_{ω→∞} σ_max(G(iω)).
if g_∞ > σ_max(G(iω_j)), j = 1, ..., ℓ then
    Set ‖G‖_{H∞} = g_∞ and ω_* = ∞.
    Return.
else
    Set ε_1 = r^est_C(E, A, B, C) as in (4.9).
    for j = 1, 2, ..., k do
        Compute α(ε_j), and right and left eigenvectors x_j and y_j associated to the
        optimal pseudopole s_j.
        Perform a Newton step: set ε_{j+1} = ε_j − α(ε_j) / (‖B^T y(ε_j)‖_2 ‖C x(ε_j)‖_2).
    end for
end if
Set ‖G‖_{H∞} = ε_{k+1}^{-1} and ω_* = Im(s_k).
```

When we assume that the $\mathcal{H}_\infty$-norm is attained at a finite frequency, we compute the root of $\alpha(\cdot)$ as described above. As the initial value we take $\varepsilon_1 = r_{\mathbb{C}}^{\mathrm{est}}(E, A, B, C)$ as in (4.9) which is already very close to the exact value of the structured stability radius for most of our examples. In our actual implementation of the algorithm we also check if the most dominant poles are purely real. In this case we assume that $\|G\|_{\mathcal{H}_\infty} = \|G(0)\|_2$ and return this value. This is done to improve the performance of the algorithm since there are many examples with this property.

6. Comparison with the Method of Guglielmi, Gürbüzbalaban, and Overton. As already pointed out in the introduction, the work [22] uses a similar idea to compute the $\mathcal{H}_\infty$-norm of transfer functions of the form

$$G(s) = C(sI_n - A)^{-1}B + D. \tag{6.1}$$

The presence of a nonzero matrix D makes the derivation and analysis of the algorithm from [22] particularly cumbersome and difficult. In this case the role of the structured ε-pseudospectra of our paper is taken by the so-called *ε-spectral value sets* which are defined by

$$\Xi_\varepsilon(A, B, C, D) := \left\{ s \in \mathbb{C} : s \in \Lambda\left(A + B\Delta(I_p - D\Delta)^{-1}C\right) \right. \\ \left. \text{for some } \Delta \in \mathbb{C}^{m\times p} \text{ with } \|\Delta\|_2 < \varepsilon \right\},$$

where $\Lambda(A)$ denotes the spectrum of a square matrix A. Then, it is shown that $\Xi_\varepsilon(A, B, C, D)$ can be constructed by only using rank-1 perturbations Δ, and therefore, also the rightmost point in the spectral value set can be realized by a rank-1 perturbation $\varepsilon u_* v_*^H$ with $\|u_*\|_2 = \|v_*\|_2 = 1$. The construction of this optimizing perturbation is done by an iteration that yields a sequence of normalized vector pairs $((u_j, v_j))_{j=0}^\infty$. For each $j > 0$, u_j and v_j are determined as solutions of the optimization problem

$$\max_{\|u\|_2=\|v\|_2=1} \mathrm{Re}\left(y_j^H B \left(\frac{uv^H}{1 - \varepsilon v^H D u} \right) C x_j \right), \tag{6.2}$$

where x_j and y_j are the right and left eigenvectors to the rightmost eigenvalue of the perturbed matrix $A + \varepsilon B u_{j-1} v_{j-1}^H (I_p - \varepsilon D u_{j-1} v_{j-1}^H)^{-1} C$, respectively. An explicit solution of this optimization problem is derived in [22]. In our paper we circumvent the solution of such an optimization problem, since we always transform the given realization into the form (1.4) to eliminate D. Then we can directly construct the next perturbation matrix by using (4.5). Of course, then we have to deal with a descriptor system, even if the original problem comes from a standard state-space system.

Note that both methods are also *not* equivalent in the context of standard state-space systems. To see this we rewrite (6.1) as

$$G(s) = \begin{bmatrix} C & I_p \end{bmatrix} \left(s \begin{bmatrix} I_n & 0 \\ 0 & 0 \end{bmatrix} - \begin{bmatrix} A & 0 \\ 0 & -I_p \end{bmatrix} \right)^{-1} \begin{bmatrix} B \\ D \end{bmatrix}.$$

Let s_0 be the rightmost finite eigenvalue of the pencil $\lambda \left[\begin{smallmatrix} I_n & 0 \\ 0 & 0 \end{smallmatrix}\right] - \left[\begin{smallmatrix} A & 0 \\ 0 & -I_p \end{smallmatrix}\right]$ with right and left eigenvectors $x_0 = \begin{bmatrix} x_{0,1}^T & x_{0,2}^T \end{bmatrix}^T$ and $y_0 = \begin{bmatrix} y_{0,1}^T & y_{0,2}^T \end{bmatrix}^T$. Then, we have $x_{0,2} = 0$ and $y_{0,2} = 0$. Therefore, the first perturbation in the descriptor system case is constructed by the vectors

$$u_0 := B^T y_{0,1} / \left\| B^T y_{0,1} \right\|_2, \quad v_0 := C x_{0,1} / \left\| C x_{0,1} \right\|_2. \tag{6.3}$$

Furthermore, since $x_{0,1}$ and $y_{0,1}$ are the right and left eigenvectors of the matrix A with respect to the eigenvalue s_0, the first perturbation in the standard system case is computed via the solution of the optimization problem (6.2) with $x_j = x_{0,1}$ and $y_j = y_{0,1}$. However, its solution only corresponds to (6.3) if $D = 0$. In our algorithm, D is completely ignored, whereas in [22] both D and ε play a certain role in the optimization process. So, even if both methods converge to the same locally rightmost point in the structured pseudospectrum or spectral value set, the path of intermediate iterates might be different. It is far from obvious to see whether one of the approaches works better than the other one, but this is also out of the scope of this paper. However, this question is particularly interesting in the context of generalizing the approach from [22] to the descriptor system case, since there is a large freedom of choosing E and D to obtain the same transfer function.

The second main difference to [22] is that in our algorithm we explicitly consider poles instead of eigenvalues. This difference seems to be of minor nature but it has some important consequences. Consider for example the case that $E = I_n$ and A is a stable matrix. Now we could inflate A by an uncontrollable or unobservable eigenvalue λ_0 to still obtain the same transfer function. Since we can choose λ_0 arbitrarily we can also place it far in the right half-plane. The method from [22] would now choose λ_0 as a starting value and directly return $\mathrm{Re}(\lambda_0)$ as spectral value set abscissa since there is no spectral value set component around λ_0. This could then lead to a wrong result, since $\mathrm{Re}(\lambda_0)$ can be much larger than the corresponding spectral value set abscissa obtained by using the original data. This problem is avoided by our method since obviously λ_0 is no pole of the transfer function. In fact it is only a removable singularity. The further incorporation of only the most dominant poles by our method enables us to find good starting values that can be used to indeed find a global instead of a local maximizer of $\|G(\mathrm{i}\cdot)\|_2$. This is not guaranteed by [22], since controllability and observability do not play a role for choosing the initial eigenvalue.

7. Numerical Results.

7.1. Test Setup. In this section we present some numerical results of our downloadable implementation*. The tests have been performed on a 2.6.32-23-generic-pae Ubuntu machine with Intel® Core™2 Duo CPU with 3.00GHz and 2GB RAM. The algorithms have been implemented and tested in MATLAB 7.14.0.739 (R2012a). To compute the (exponentially) dominant poles we use a (slightly modified) version of Rommes' MATLAB codes†. The data for the numerical examples was taken from [15, 21, 34, 43] and it can also be downloaded from Rommes' website or from the SLICOT page‡. As dominance measure we use (4.7). In Subsection 7.3 we also analyze the behavior of the algorithm using the exponential dominance measure. The tolerance on the relative change of the iterates in Algorithm 1 is set to $\tau = 10^{-3}$. We also abort the iteration when the iterates start to cycle which typically happens when they are approaching zero. In Algorithm 2 we abort this iteration when the relative change of the iterates is below 10^{-6}, i.e., if $\left|1 - \frac{\varepsilon_k}{\varepsilon_{k+1}}\right| < 10^{-6}$. To obtain $r_{\mathbb{C}}^{\text{est}}(E, A, B, C)$, we compute 20 dominant poles using SAMDP (40 for the `peec` example and 30 for the `bips07_1693` system). For every further outer iteration we compute only 5 dominant poles (10 for the `peec` example). Note that we have to compute more dominant poles for `peec` and `bips07_1693` to ensure that the most dominant poles are really found. Both examples are particularly difficult, so it is necessary to deviate from the default values mentioned above.

7.2. Test Results. In Table 7.1 we summarize the results of 33 numerical tests. The first 13 examples are standard or generalized state space systems whereas the other 20 ones are descriptor systems (with singular E). With n_{outer} we denote the number of outer iterations, i.e., the number of steps needed by Algorithm 2 to find the root. By n_{inner} we refer to the total number of inner iterations, i.e., the total number of steps needed by Algorithm 1.

For all tests, the correct value of $\|G\|_{\mathcal{H}_\infty}$ was found. In 30 tests the first outer iteration returned a positive value. However, for 3 of the tests (`M10PI_n1`, `M10PI_n`, `bips07_1693`), a negative value was returned and therefore, we have to try more dominant poles (one for each `M10PI_n1`, `M10PI_n` and four for `bips07_1693`) to converge to the correct initial value.

For a more detailed impression of the behavior of the algorithm, Tables 7.2 and 7.3 summarize the convergence history for the `M20PI_n` and the `bips07_2476` examples, listing each intermediate iterate for each iteration of the root-finding algorithm. We clearly observe a linear convergence of Algorithm 1 with different convergence rates depending on the problem, see also Subsection 4.5.

In Figure 7.1 we also depict a set of structured pseudospectra for the `M20PI_n` example and the iterates of the first iteration of Algorithm 1. Blue contours in Figure 7.1(a) correspond to small perturbation levels whereas yellow and red contours indicate areas which need larger perturbations to be reached by the perturbed poles. Therefore, poles that correspond to the blue contours are particularly controllable and observable. Intuitively, it is clear that the $\mathcal{H}_\infty$-norm will most likely be attained at frequencies close to these poles. This is also confirmed by having a look at Figure 7.2 that shows transfer function plots for the `M20PI_n` and `bips07_2476` examples together with the computed $\mathcal{H}_\infty$-norms. For the `M20PI_n` example we observe that the correct norm value is computed even though there are lots of close-by peaks of similar

*`http://www.mpi-magdeburg.mpg.de/mpcsc/software/infnorm/`

†`http://sites.google.com/site/rommes/software`

‡`http://www.slicot.org/index.php?site=benchmodred`

Table 7.1: Numerical results for 33 test examples

#	example	n	m	p	$\|G\|_{\mathcal{H}_\infty}$	ω_*	$\alpha_{r^{\mathrm{f}}_{\mathbb{C}}}(E,A,B,C)$	n_{outer}	n_{inner}	time in s
1	build	48	1	1	5.27633e-03	5.20608e+00	4.3258e-15	3	13	1.54
2	pde	84	1	1	1.08358e+01	0	-1.4872e-15	1	6	2.08
3	CDplayer	120	2	2	2.31982e+06	2.25682e+01	8.6683e-16	2	8	2.70
4	iss	270	3	3	1.15887e-01	7.75093e-01	7.1406e-17	1	3	2.69
5	beam	348	1	1	4.55487e+03	1.04575e-01	-2.0176e-13	2	8	50.22
6	S10PI_n1	528	1	1	3.97454e+00	7.53151e+03	3.6808e-11	2	7	1.78
7	S20PI_n1	1028	1	1	3.44317e+00	7.61831e+03	4.0418e-13	3	13	4.22
8	S40PI_n1	2028	1	1	3.34732e+00	6.95875e+03	1.9663e-12	2	8	4.77
9	S80PI_n1	4028	1	1	3.37016e+00	6.96149e+03	1.3880e-12	2	8	10.50
10	M10PI_n1	528	3	3	4.05662e+00	7.53181e+03	3.3271e-12	3	11	3.08
11	M20PI_n1	1028	3	3	3.87260e+00	5.06412e+03	1.0967e-12	2	8	3.63
12	M40PI_n1	2028	3	3	3.81767e+00	5.07107e+03	5.9180e-13	2	8	5.83
13	M80PI_n1	4028	3	3	3.80375e+00	5.07279e+03	3.7053e-13	2	8	10.88
14	peec	480	1	1	3.52651e-01	5.46349e+00	-1.8202e-10	2	7	20.80
15	S10PI_n	682	1	1	3.97454e+00	7.53151e+03	3.8015e-11	2	7	2.29
16	S20PI_n	1182	1	1	3.44317e+00	7.61831e+03	-4.3232e-13	3	13	4.67
17	S40PI_n	2182	1	1	3.34732e+00	6.95875e+03	1.0369e-12	2	8	5.35
18	S80PI_n	4182	1	1	3.37016e+00	6.96149e+03	-6.3127e-14	2	8	10.41
19	M10PI_n	682	3	3	4.05662e+00	7.53181e+03	1.4553e-12	3	11	3.56
20	M20PI_n	1182	3	3	3.87260e+00	5.06412e+03	-1.8303e-13	2	8	4.03
21	M40PI_n	2182	3	3	3.81767e+00	5.07107e+03	8.4266e-13	2	8	6.11
22	M80PI_n	4182	3	3	3.80375e+00	5.07279e+03	1.5073e-12	2	8	11.28
23	bips98_606	7135	4	4	2.01956e+02	3.81763e+00	2.6525e-14	3	13	35.43
24	bips98_1142	9735	4	4	1.60427e+02	4.93005e+00	1.1867e-13	3	22	69.65
25	bips98_1450	11305	4	4	1.97389e+02	5.64575e+00	1.2481e-14	3	16	61.65
26	bips07_1693	13275	4	4	2.04168e+02	5.53766e+00	2.1761e-12	7	45	167.10
27	bips07_1998	15066	4	4	1.97064e+02	6.39968e+00	4.8834e-13	2	20	102.11
28	bips07_2476	16861	4	4	1.89579e+02	5.88971e+00	4.7231e-11	2	30	146.18
29	bips07_3078	21128	4	4	2.09445e+02	5.55792e+00	1.5001e-13	3	13	91.05
30	xingo_afonso_itaipu	13250	1	1	4.05605e+00	1.09165e+00	-4.1368e-14	2	7	39.24
31	mimo8x8_system	13309	8	8	5.34292e-02	1.03313e+00	2.4820e-12	2	14	78.47
32	mimo28x28_system	13251	28	28	1.18618e-01	1.07935e+00	6.1195e-14	2	9	85.36
33	mimo46x46_system	13250	46	46	2.05631e+02	1.07908e+00	4.8454e-14	2	8	115.91

Table 7.2: Convergence history for the `M20PI_n` example

	k	
	1	2
$\mathrm{Re}(\lambda_{\mathrm{dom}})$	-6.7945e-02	1.6145e-08
	2.3140e-03	1.6256e-08
	3.0285e-03	1.6257e-08
	3.0355e-03	—
	3.0356e-03	—
ε_k	2.58250e-01	2.58224e-01

Table 7.3: Convergence history for the `bips07_2476` example

	k	
	1	2
$\mathrm{Re}(\lambda_{\mathrm{dom}})$	-8.1617e-02	2.1202e-08
	-9.6637e-03	3.0116e-08
	-2.6717e-03	3.4986e-08
	-9.8184e-04	3.7652e-08
	-3.9561e-04	3.9111e-08
	-1.5362e-04	3.9910e-08
	-4.3525e-05	4.0348e-08
	9.6185e-06	4.0587e-08
	3.6273e-05	4.0718e-08
	4.9989e-05	4.0790e-08
	5.7173e-05	4.0830e-08
	6.0984e-05	—
	6.3022e-05	—
	6.4120e-05	—
	6.4714e-05	—
	6.5036e-05	—
	6.5211e-05	—
	6.5307e-05	—
	6.5359e-05	—
ε_k	5.27515e-03	5.27485e-03

height. We can also see that lots of peaks are introduced in the transfer function at frequencies that correspond to areas that are covered by the blue contours in Figure 7.1(a).

7.3. Comparison of Dominance Measures. Since our exponential dominance measure is a heuristic method, we provide some results that emphasize that using (4.8) with larger values of β as an alternative dominance measure can also be a good choice. In particular, we perform a study of the behavior of our algorithm for different values of β, but also with the standard measure given by (4.7). To ensure that the most exponentially dominant poles are really found in the inner iterations we increase n_{inner} to 20, but all other options are the same as before. In Table 7.4

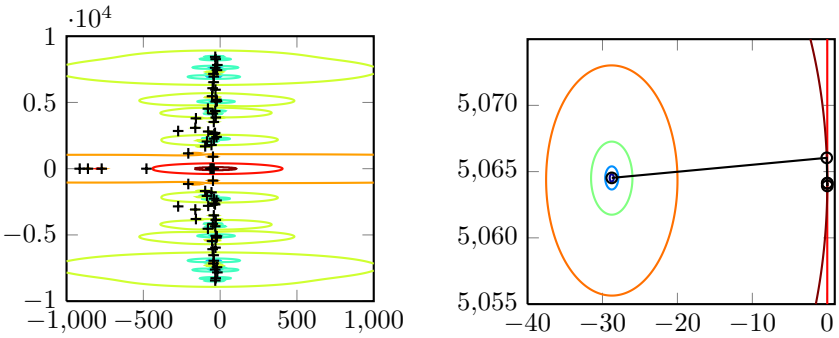

(a) Structured pseudospectra (b) Iterates of the first outer iteration

Fig. 7.1: Structured pseudospectra with most controllable/observable poles (black pluses) and first outer iteration for the `M20PI_n` example

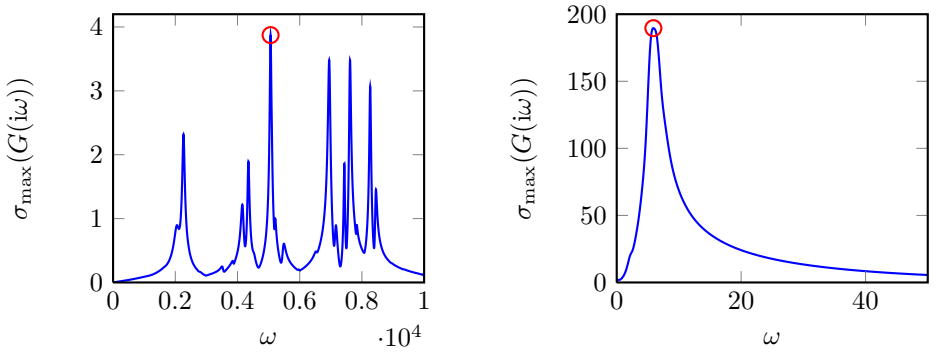

(a) `M20PI_n` (b) `bips07_2476`

Fig. 7.2: Transfer function plots for the `M20PI_n` and `bips07_2476` test examples with computed $\mathcal{H}_\infty$-norm (red circle)

we list those examples that fail when trying to compute the $\mathcal{H}_\infty$-norm using different dominance measures. Unfortunately, for all tested values of β, some of the examples fail which is always due to a wrong selection of the poles with the respective dominance measure. Nevertheless, also all examples could be solved for some choice of β. For the `iss` example, we obtain $\|G\|_{\mathcal{H}_\infty} = 0.115885$ for $\beta = 10$ and $\beta = 100$ which is slightly smaller than the true value. This inaccuracy is also related to a different pole selection in the iteration for different dominance measures. However, the algorithm converges to the same peak in the transfer function.

In conclusion, it is important to choose a good value of β *depending on the actual example* when applying (4.8). The table also makes clear that it is advisable to put a rather high weight on the real part of the poles which corresponds to a high value of β. However, it is still important to have an eye on the perturbability of the poles which is neglected if β becomes too large. The standard measure (4.7) works particularly well for our examples since the computed dominant poles already give very good initial estimates of the actual value of the $\mathcal{H}_\infty$-norm. However, if this is not the case, the

Table 7.4: Comparison of different dominance measures for the 33 test examples from Table 7.1

dominance measure	failed examples
(4.7)	—
(4.8) with $\beta = 1$	`iss`, `peec`, `bips98_606`, `bips98_1142`, `bips98_1450`, `bips07_1693`, `xingo_afonso_itaipu`, `mimo8x8_system`, `mimo46x46_system`
(4.8) with $\beta = 10$	(`iss`), `peec`
(4.8) with $\beta = 100$	(`iss`), `peec`
(4.8) with $\beta = 1000$	`peec`
(4.8) with $\beta = 10000$	`M10PI_n1`, `M10PI_n`

Table 7.5: Comparison of the new method with standard approaches

	computed $\mathcal{H}_\infty$-norm			time in s		
example	`norm`	`AB13HD`	new method	`norm`	`AB13HD`	new method
`M10PI_n`	4.05662	4.05662	4.05662	40.44	50.59	3.56
`M20PI_n`	**9.92404**	3.87260	3.87260	296.65	276.41	4.03
`M40PI_n`	3.81766	3.81767	3.81767	2322.66	1998.26	6.11

rightmost pseudopole in the first iteration might be "far" in the right half-plane which makes the exponential dominance measure more advisable.

7.4. Comparison with Other Methods. This subsection gives a brief comparison with other methods, in particular those based on the solution of Hamiltonian eigenvalue problems. These are implemented in the MATLAB Control Systems Toolbox as the function `norm` and in the Systems and Control Library SLICOT[§] as the upcoming subroutine `AB13HD`. Both implementations rely on dense matrix algebra and therefore, they do not exploit the *sparse structure* of the involved matrices. We illustrate the speed-up of the method compared to the standard approaches in Table 7.5 for some smaller examples that can be solved by all available implementations. Both, the MATLAB function `norm` and SLICOT's `AB13HD` are used with a relative tolerance of 10^{-6} to obtain a similar accuracy as in Table 7.1. The SLICOT solver is compiled using `gfortran` with option `-O2` and the latest versions of LAPACK and BLAS (v3.4.1). From the table we conclude that the new method is much faster than existing algorithms. A high speed-up can already be observed for small and medium-sized examples. Furthermore, for the `M20PI_n` example, the new method and the SLICOT solver `AB13HD` are able to compute the correct result whereas the MATLAB solver `norm` returns the wrong norm value without printing an error or warning message.

Furthermore, we compare our approach with the method in [22] for standard state-space examples. The MATLAB code for [22] is freely available[¶]. As examples we use the state-space examples used in Table 7.1 (#1–5). Moreover, we generated test systems using state matrices A from EigTool [48] or the COMPl$_e$ib package [32, 33] with randomly generated sparse input and output matrices B and C and

[§] `http://www.slicot.org/`

[¶] `http://cims.nyu.edu/~mert/software/hinfinity.html`

Table 7.6: Comparison of our method with [22] for standard state-space systems

#	example	n	m	p	computed $\mathcal{H}_\infty$-norm		time in s	
					[22]	new meth.	[22]	new meth.
1	`build`	48	1	1	5.27633e-03	5.27633e-03	0.93	1.54
2	`pde`	84	1	1	1.08358e+01	1.08358e+01	0.99	2.08
3	`CDplayer`	120	2	2	2.31982e+06	2.31982e+06	9.68	2.70
4	`iss`	270	3	3	**1.20261e-02**	1.15887e-01	5.53	2.69
5	`beam`	348	1	1	4.55487e+03	4.55487e+03	10.97	50.22
6	`convdiff_fd`	400	4	6	**1.46898e+01**	1.46968e+01	1247.09	92.21
7	`dwave`	2048	4	6	1.27874e+01	1.27874e+01	58.34	5.55
8	`HF1`	130	1	2	8.42158e-01	8.42158e-01	1.15	0.34
9	`markov`	5050	4	6	3.37266e+00	3.37266e+00	98.70	14.56
10	`NN18`	1006	1	2	9.29638e+00	**fail**	63.84	—
11	`olmstead`	500	4	6	2.79331e+00	2.79331e+00	23.17	1.68
12	`tolosa`	4000	4	6	**fail**	6.76382e+01	—	15.40

random feedthrough matrix D. For a good comparison we choose similar termination tolerances in both methods. For our algorithm we use the same tolerances as above. For the method from [22] we choose tolerances for the relative and absolute error of 10^{-6} and 10^{-12}, respectively. As tolerance of the absolute error of the spectral value set abscissa computation we take 10^{-3}. In order to apply our method, we first transform a system with $D \neq 0$ into the form (1.3). Furthermore, we remark that we let the algorithm from [22] run using *dense* arithmetics in case that $n \leq 500$ since its performance is much better in this situation. The computed $\mathcal{H}_\infty$-norms and the runtimes of the algorithms are listed in Table 7.6. First, we see that for both algorithms there are examples that could not be solved which is emphasized by boldface font in the table. For the `iss` system this is caused by convergence to a locally but not globally rightmost pseudopole whereas for `NN18` and `tolosa`, SAMDP or `eigs` from MATLAB fail, respectively. The `convdiff_fd` system is difficult in the sense that we need to increase the relative tolerance of the inner iteration of our algorithm to at least 10^{-4} to obtain an accurate result. On the other hand, even decreasing the tolerance of the absolute error of the spectral value set abscissa computation in the algorithm from [22] does not improve the accuracy of the result in Table 7.6 which is obtained by using a tolerance of 10^{-3}.

Concerning the runtimes there is no pattern observable. There are examples for which the method from [22] performs better but on the other hand there are many examples for which our method is faster. This is particularly true for those systems whose $\mathcal{H}_\infty$-norm is attained at $\omega = 0$. These are `dwave`, `HF1`, `markov`, and `olmstead`. When all dominant poles are purely real, our algorithm directly returns $\|G\|_{\mathcal{H}_\infty} = \|G(0)\|_2$ as result whereas this property is not explicitly checked by algorithm [22] which performs the full iteration. This is a particular advantage of our method since by employing the residues of the poles we can get information about the shape of the transfer function which is not possible by looking only at the location of the eigenvalues as in [22].

7.5. Limitations of the Method. In this subsection we explain limitations of our method. For illustrate these we use the `peec` example. We plotted the transfer

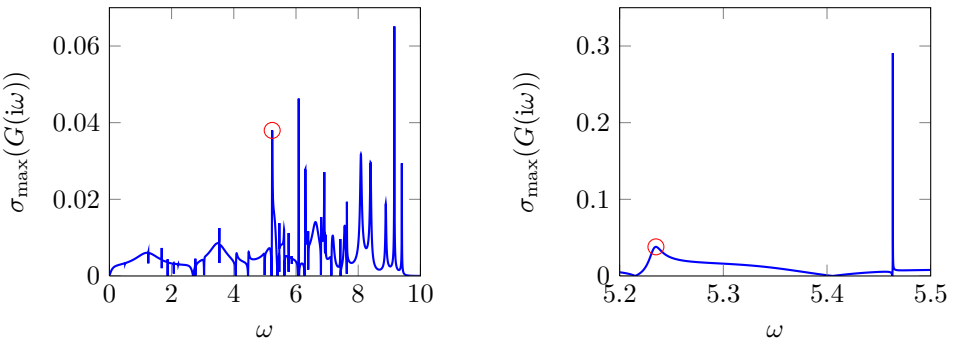

(a) Interval $(0, 10)$ (not all peaks are captured due to plotting resolution)

(b) Zoom into the interval $(5.2, 5.5)$

Fig. 7.3: Transfer function plots for the `peec` example with computed (wrong) $\mathcal{H}_\infty$-norm

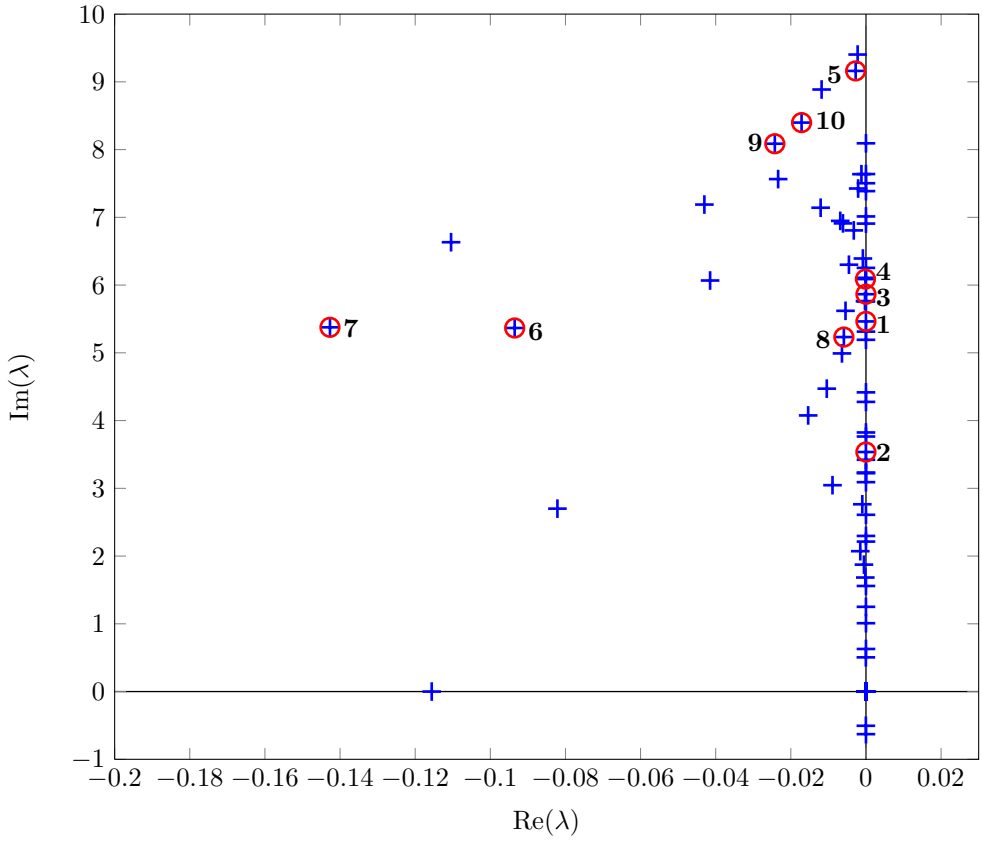

Fig. 7.4: Eigenvalues of $\lambda E - A$ for the `peec` example (blue pluses) and the 10 most dominant poles (red circles)

function of this example in Figure 7.3, once in the interval $(0, 10)$ and once for the interval $(5.2, 5.5)$, where the maximum peak is located. First of all we see, the transfer function has lots of peaks which is due to the high amount of poles close to the imaginary axis. We plot the eigenvalues of the corresponding pencil $\lambda E - A$ in Figure 7.4, together with the ten most dominant poles. It is very hard for SAMDP to find the most dominant pole. In fact, if we only compute 20 dominant poles, the actually most dominant one is not found. This is only the case if we increase the number of wanted poles up to 40. Another problem is that the maximum peak is extremely thin and spiky (see Figure 7.3(b)). We do not even see it with the resolution used for plotting Figure 7.3(a). To find it we would actually need very good approximations to the eigenvectors which are needed to construct the *optimal* rank-1 perturbation. This is only the case if we initialize the iteration with the most dominant pole and take an appropriate dominance measure to continue with the most dominant poles in each further iteration as done in Table 7.1. On the other hand, even if we start from a pole very close to this optimal pole, e.g., when we only compute 20 dominant poles and take, e.g., $\beta = 100$ in the beginning, our initial eigenvectors (the ones of the initial pencil) are not that good. Therefore, we only find the close-by peak which is much "wider" than the one we actually seek, see also the computed norm value in Figure 7.3. However, we can check if the computed norm value is larger than the 2-norms of the transfer function evaluated at the test frequencies. For this example, the test that we have implemented, is not satisfied and therefore, we can at least return an error indicator. The main problem of our method is that the user has to provide certain parameters to the algorithm, for instance the number of dominant poles that should be computed in the beginning and every further iteration, since a high number can be necessary in order to find the most dominant pole.

Unfortunately, there also exist examples for which we observe an extremely slow convergence of SAMDP, in particular for those that have all real poles. Typically, the circuit examples from the `MNA` group of [15] are of this kind. However, for these problems, the $\mathcal{H}_\infty$-norm is attained at zero, i.e., $\|G\|_{\mathcal{H}_\infty} = \|G(0)\|_2$, see [40]. This behavior is captured by our algorithm by returning this value if the most dominant poles are all real, provided that SAMDP is able to compute the poles.

8. Conclusions and Future Research Perspectives. In this paper we have introduced a new iterative scheme for computing the $\mathcal{H}_\infty$-norm of a transfer function. This routine uses the relationship between the $\mathcal{H}_\infty$-norm and the structured complex stability radius of a matrix or a pencil. Based on the method introduced in [26], the algorithm computes a sequence of structured pseudospectral abscissae. This is done by computing an optimal rank-1 perturbation of the system such that one of the eigenvalues of the perturbed matrix or pencil converges to the rightmost structured pseudopole of the transfer function.

This algorithm can also be seen as a basis to solve certain related problems for descriptor systems. For instance one could think of a discrete-time version of the algorithm presented here. This has already been done in [22] via optimizing the structured pseudospectral radius. However, the authors of [22] have not used a method that takes controllability or observability of the poles into account. It is an open problem to develop and implement a dominant pole algorithm for the discrete-time case to employ similar ideas as presented in this paper. Another future research direction could be on the analysis of *real* structured stability radii. Most likely, this will also lead to an optimization procedure over rank-2 perturbations as presented in [24]. Another problem that we want to address in the future is the computation of

the passivity radius [37] of a large-scale dynamical system. This problem relates to pseudospectra of Hamiltonian matrices and pencils. As shown in [23] there is also a low-rank dynamics for general Hamiltonian perturbations. However, for the passivity radius, the perturbation structure is more specific, so one has to find a different approach for this particular problem.

Acknowledgment. We thank Volker Mehrmann from TU Berlin for pointing at the difficulties arising if the perturbations make the transfer functions improper or not well-defined. We gratefully acknowledge the work done by our former intern Maximilian Bremer from the University of Texas at Austin by implementing a MATLAB code for the visualization of structured pseudospectra. Furthermore, we thank the two anonymous reviewers for their valuable and constructive comments that helped to significantly improve the quality of the paper.

REFERENCES

[1] P. Benner, R. Byers, V. Mehrmann, and H. Xu, *Numerical computation of deflating subspaces of skew-Hamiltonian/Hamiltonian pencils*, SIAM J. Matrix Anal. Appl., 24 (2002), pp. 165–190.

[2] P. Benner, J. Saak, F. Schieweck, P. Skrzypacz, and H. K. Weichelt, *A non-conforming composite quadrilateral finite element pair for feedback stabilization of the Stokes equations*, J. Numer. Math., (2012). Accepted, also available as Max Planck Institute Magdeburg Preprint MPIMD/12-19.

[3] P. Benner, V. Sima, and M. Voigt, *$\mathcal{L}_\infty$-norm computation for continuous-time descriptor systems using structured matrix pencils*, IEEE Trans. Automat. Control, 57 (2012), pp. 233–238.

[4] ———, *Robust and efficient algorithms for $\mathcal{L}_\infty$-norm computation for descriptor systems*, in Proceedings of the 7th IFAC Symposium on Robust Control Design, Aalborg, Denmark, June 2012, IFAC, pp. 195–200.

[5] P. Benner and M. Voigt, *$\mathcal{H}_\infty$-norm computation for large and sparse descriptor systems*, Proceedings in Applied Mathematics and Mechanics, 12 (2012), pp. 797–800.

[6] ———, *Numerical computation of structured complex stability radii od large-scale matrices and pencils*, in Proceedings of the 51st IEEE Conference on Decision and Control, Maui, Hawaii, USA, Dec. 2012, pp. 6560–6565.

[7] S. Boyd and V. Balakrishnan, *A regularity result for the singular values of a transfer matrix and a quadratically convergent algorithm for computing its L_∞-norm*, Systems Control Lett., 15 (1990), pp. 1–7.

[8] S. Boyd, V. Balakrishnan, and P. Kabamba, *A bisection method for computing the H_∞ norm of a transfer matrix and related problems*, Math. Control Signals Systems, 2 (1989), pp. 207–219.

[9] N. A. Bruinsma and M. Steinbuch, *A fast algorithm to compute the H_∞-norm of a transfer function matrix*, Systems Control Lett., 14 (1990), pp. 287–293.

[10] J. V. Burke, A. S. Lewis, and M. L. Overton, *Robust stability and a criss-cross algorithm for pseudospectra*, IMA J. Numer. Anal., 23 (2003), pp. 359–375.

[11] R. Byers, *A bisection method for measuring the distance of a stable matrix to the unstable matrices*, SIAM J. Sci. Stat. Comput., 9 (1988), pp. 875–881.

[12] R. Byers and N. K. Nichols, *On the stability radius of a generalized state-space systems*, Linear Algebra Appl., 188–189 (1993), pp. 113–134.

[13] Y. Chahlaoui, K. Gallivan, and P. Van Dooren, *$\mathcal{H}_\infty$-norm calculations of large sparse systems*, in Proceedings of the International Symposium of Mathematical Theory of Networks and Systems, Leuven, Belgium, 2004.

[14] ———, *Calculating the $\mathcal{H}_\infty$ norm of a large sparse system via Chandrasekhar iterations and extrapolation*, in ESAIM Proceedings, vol. 20, Rabat, Algeria, Oct. 2007, pp. 83–92.

[15] Y. Chahlaoui and P. Van Dooren, *A collection of benchmark examples for model reduction of linear time invariant dynamical systems*, tech. report, Feb. 2002. SLICOT Working Note 2002–2.

[16] L. Dai, *Singular Control Systems*, vol. 118 of Lecture Notes in Control and Inform. Sci., Springer-Verlag, Heidelberg, 1989.

[17] N. H. Du, *Stability radii of differential algebraic equations with structured perturbations*, Systems Control Lett., 57 (2008), pp. 546–553.
[18] N. H. Du, V. H. Linh, and V. Mehrmann, *Robust stability of differential-algebraic equations*, in Surveys in Differential-Algebraic Equations I, A. Ilchmann and T. Reis, eds., Differential-Algebraic Equations Forum, Springer-Verlag, Berlin, Heidelberg, 2013, ch. 2, pp. 63–95.
[19] N. H. Du, D. D. Thuan, and N. C. Liem, *Stability radius of implicit dynamic equations with constant coefficients on time scales*, Systems Control Lett., 60 (2011), pp. 596–603.
[20] E. Eich-Soellner and C. Führer, *Numerical Methods in Multibody Dynamics*, B. G. Teubner, Stuttgart, 1998.
[21] F. Freitas, J. Rommes, and N. Martins, *Gramian-based reduction method applied to large sparse power system descriptor models*, IEEE Trans. Power Syst., 23 (2008), pp. 1258–1270.
[22] N. Guglielmi, M. Gürbüzbalaban, and M. L. Overton, *Fast approximation of the H_∞ norm via optimization of spectral value sets*, SIAM J. Matrix Anal. Appl., 34 (2013), pp. 709–737.
[23] N. Guglielmi, D. Kressner, and C. Lubich, *Low-rank differential equations for Hamiltonian matrix nearness problems*, Oberwolfach Preprint OWP 2013–01, Mathematisches Forschungsinstitut Oberwolfach, Jan. 2013. Available from `http://www.mfo.de/scientific-programme/publications/owp/2013/OWP2013_01.pdf`.
[24] N. Guglielmi and C. Lubich, *Low-rank dynamics for computing extremal points of real pseudospectra*, SIAM J. Matrix Anal. Appl., (2013). In press.
[25] N. Guglielmi and M. L. Overton, *Local convergence analysis of [22] – private communication with M. L. Overton.*
[26] ———, *Fast algorithms for the approximation of the pseudospectral abscissa and pseudospectral radius of a matrix*, SIAM J. Matrix Anal. Appl., 32 (2011), pp. 1166–1192.
[27] M. Heinkenschloss, D. C. Sorensen, and K. Sun, *Balanced truncation model reduction for a class of descriptor systems with application to the Oseen equations*, SIAM J. Sci. Comput., 30 (2008), pp. 1038–1063.
[28] D. Hinrichsen and A. J. Pritchard, *Stability radii of linear systems*, Systems Control Lett., 7 (1986), pp. 1–10.
[29] ———, *Stability radius for structured perturbations and the algebraic Riccati equation*, Systems Control Lett., 8 (1986), pp. 105–113.
[30] ———, *Real and Complex Stability Radii: A Survey*, vol. 6 of Progress in Systems and Control Theory, Birkhäuser, Boston, 1990, pp. 119–162.
[31] P. Kunkel and V. Mehrmann, *Differential-Algebraic Equations - Analysis and Numerical Solution*, Textbooks in Mathematics, European Mathematical Society, 2006.
[32] F. Leibfritz, *Compl$_e$ib: Constraint matrix-optimization problem library – a collection of test examples for nonlinear semidefinite programs, control system design and related problems*, tech. report, 2004. Available from `http://www.friedemann-leibfritz.de/COMPlib_Data/COMPlib_Main_Paper.pdf`.
[33] F. Leibfritz and W. Lipinski, *Compl$_e$ib 1.0 – user manual and quick reference*, tech. report, 2004. Available from `http://www.friedemann-leibfritz.de/COMPlib_Data/COMPlib_User_Guide.pdf`.
[34] N. Martins, P. C. Pellanda, and J. Rommes, *Computation of transfer function dominant zeros with applications to oscillation damping control of large power systems*, IEEE Trans. Power Syst., 22 (2007), pp. 1657–1664.
[35] V. Mehrmann, C. Schröder, and V. Simoncini, *An implicitly-restarted Krylov subspace method for real symmetric/skew-symmetric eigenproblems*, Linear Algebra Appl., 436 (2012), pp. 4070–4087.
[36] V. Mehrmann and T. Stykel, *Balanced truncation model reduction for large-scale systems in descriptor form*, in Dimension Reduction of Large-Scale Systems, P. Benner, V. Mehrmann, and D. Sorensen, eds., vol. 45 of Lecture Notes Comput. Sci. Eng., Springer-Verlag, Berlin, Heidelberg, New York, 2005, ch. 3, pp. 89–116.
[37] M. L. Overton and P. Van Dooren, *On computing the complex passivity radius*, in Proc. 44th IEEE Conference on Decision and Control, and the European Control Conference 2005, Dec. 2005, pp. 7960–7964.
[38] T. Reis, *Circuit synthesis of passive descriptor systems – a modified nodal approach*, Int. J. Circ. Theor. Appl., 38 (2010), pp. 44–68.
[39] T. Reis and T. Stykel, *PABTEC: Passivity-preserving balanced truncation for electrical circuits*, IEEE Trans. Computer-Aided Design Integr. Circuits Syst., 29 (2010), pp. 1354–1367.
[40] ———, *Lyapunov balancing for passivity-preserving model reduction of RC circuits*, SIAM J. Appl. Dyn. Syst., 10 (2011), pp. 1–34.
[41] K. S. Riedel, *Generalized epsilon-pseudospectra*, SIAM J. Numer. Anal., 31 (1994), pp. 1219–

1225.
[42] J. Rommes, *Arnoldi and Jacobi-Davidson methods for generalized eigenvalue problems $Ax = \lambda Bx$ with singular B*, Math. Comp., 77 (2008), pp. 995–1015.
[43] J. Rommes and N. Martins, *Efficient computation of multivariate transfer function dominant poles using subspace acceleration*, IEEE Trans. Power Syst., 21 (2006), pp. 1471–1483.
[44] ———, *Efficient computation of transfer function dominant poles using subspace acceleration*, IEEE Trans. Power Syst., 21 (2006), pp. 1218–1226.
[45] J. Rommes and G. L. G. Sleijpen, *Convergence of the dominant pole algorithm and Rayleigh quotient iteration*, SIAM J. Matrix Anal. Appl., 30 (2008), pp. 346–363.
[46] G. W. Stewart and J.-G. Sun, *Matrix Perturbation Theory*, Computer Science and Scientific Computing, Academic Press, 1990.
[47] J. Weickert, *Applications of the Theory of Differential-Algebraic Equations to Partial Differential Equations of Fluid Dynamics*, PhD thesis, Chemnitz University of Technology, Department of Mathematics, Germany, 1997.
[48] T. G. Wright, *Eigtool*, 2002. Available from `http://www.comlab.ox.ac.uk/pseudospectra/eigtool/`.
[49] K. Zhou and J. D. Doyle, *Essentials of Robust Control*, Prentice Hall, 1st ed., 1998.